10th Hellenic Astronomical Conference, Ioannina 5-8 Sep 2011

Magnetic activity on the Sun

Prof. Alan Hood
&
Dr. Vasilis Archontis
Royal Society, URF

University of St Andrews, UK

Overview

1. Recent observations of the Sun.

2. Solar Magnetic Activity: theoretical and numerical approach.

3. Magnetic Flux emergence: a building block of Solar Magnetic Activity.

4. Dynamic phenomena
   - Unloading of mass
   - Reconnection and coronal flux ropes
   - Eruptions
   - Sigmoids, jets and plasmoids
   - Complexity and heating.

Solar Observatories

1. SDO
   - AIA (Atmospheric Imaging Assembly) Data includes full disk images of the Sun in 10 wavelengths every 10 seconds.
   - HMI (Helioseismic and Magnetic Imager) Full-disk coverage at higher spatial resolution and vector magnetograms.
   - EVE (Extreme ultraviolet Variablity Experiment) Solar irradiance with unprecedented spectral and temporal resolution.
2. Hinode
   - SOT (Solar Optical Telescope) 0.2 arcseconds and vector magnetograms.
   - XRT (Solar X-Ray Telescope) 1.0 arcsecond in soft X-rays.
   - EIS (Extreme Ultraviolet Imaging Spectrometer).
3. Stereo
4. TRACE
5. Soho
6. RHESSI
7. Ground-based observatories (optical, H-alpha, radio mainly)

SDO - Full Disk

Excellent temperature coverage.

SDO – X Class flare I

Full disk and close-up of Active Region.

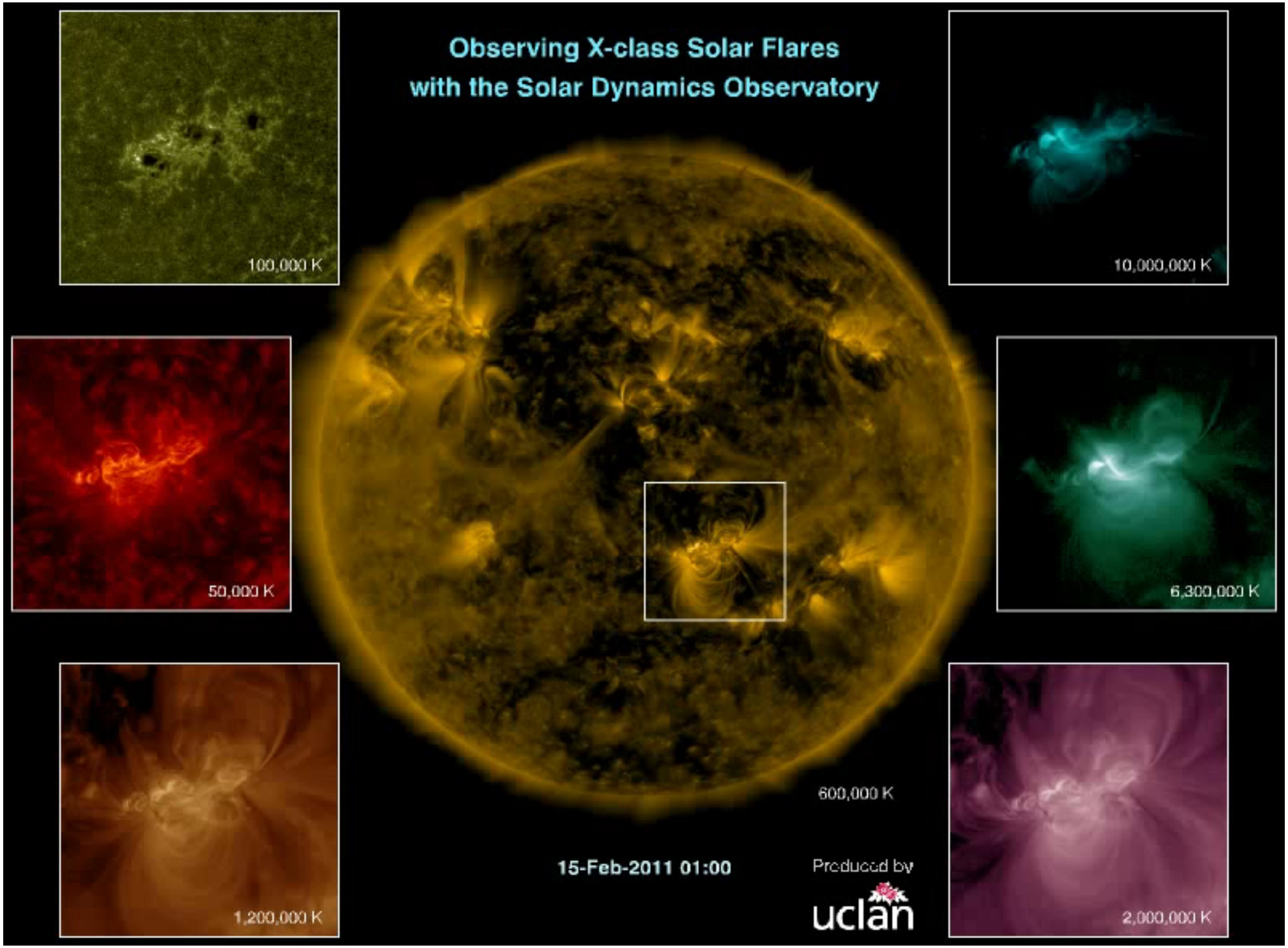

SDO – X Class flare II

Coronal temperatures and magnetograms. Sunspots and interactions.

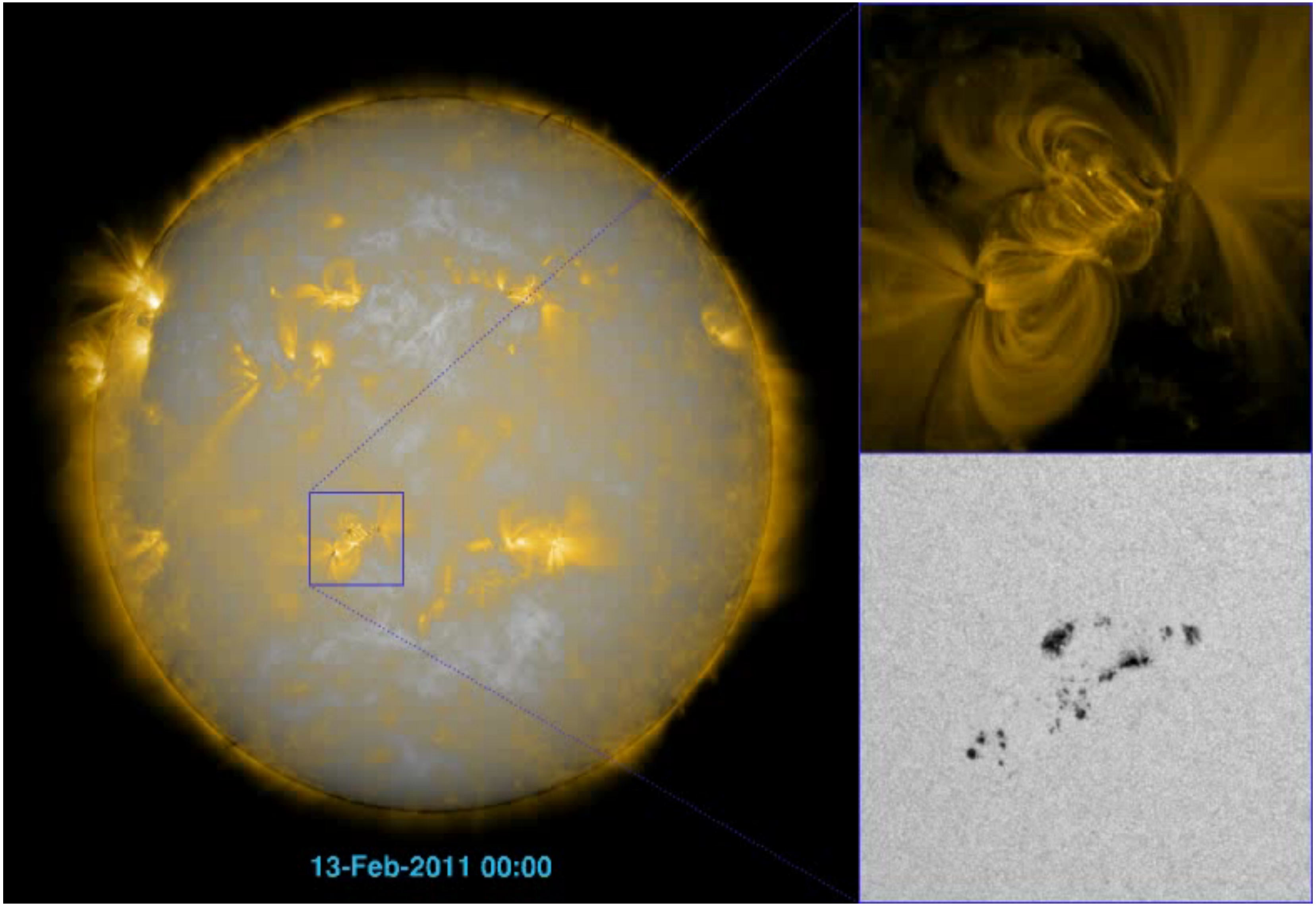

SDO – Prominence eruption

‘Cool’ and hot magnetized plasma.

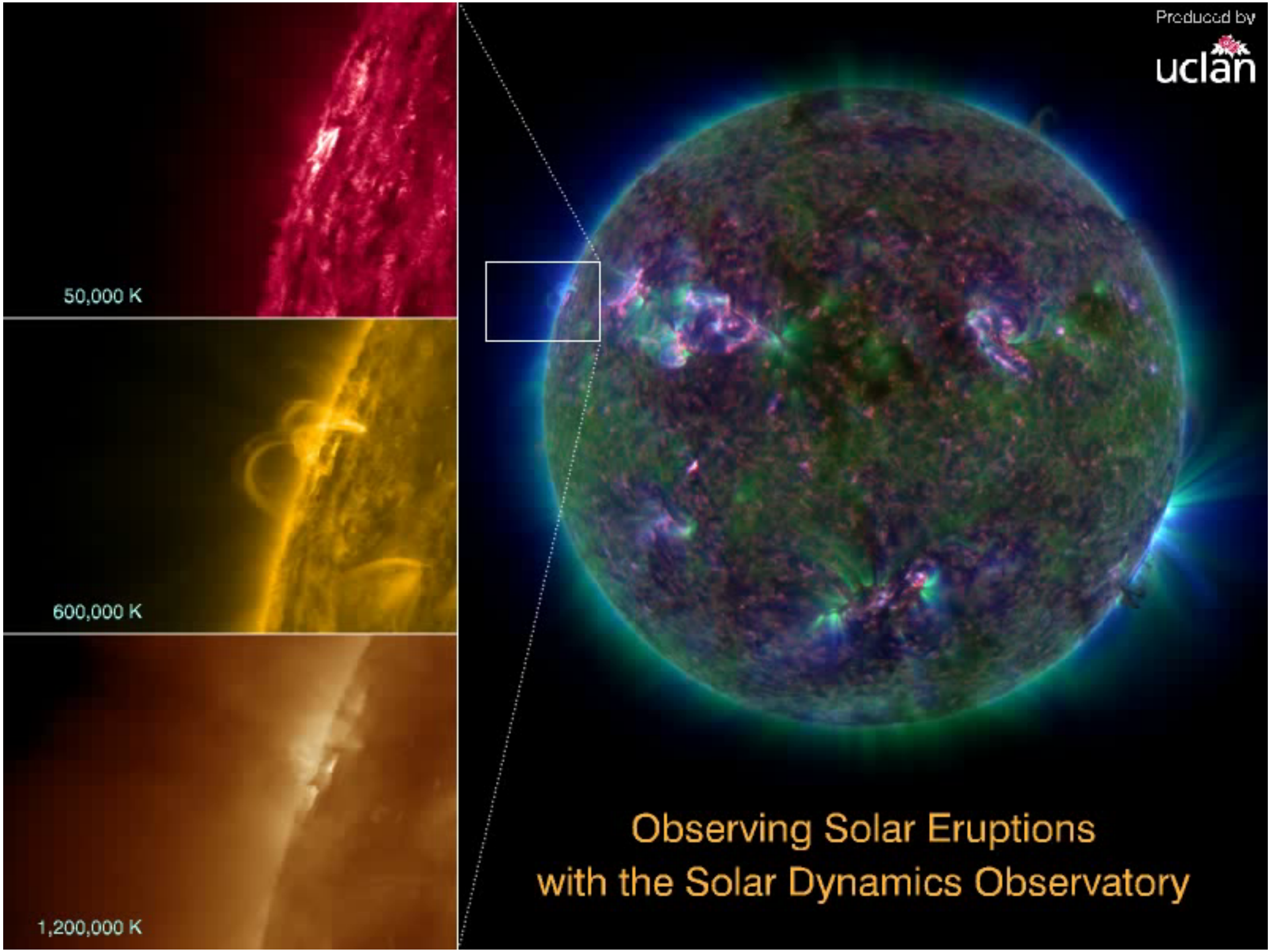

The Hel.A.S contribution

- Active regions and sunspots (Alissandrakis, Vlahos,..)
- Coronal Heating (Georgoulis, Patsourakos,Vlahos,..)
- Flux Emergence (Archontis, Georgoulis,..)
- Outflows, spicules and jets (Gontikakis, Tsinganos, Tsiropoula, Tziotziou,..).
- Prominence eruptions and CMEs (Nindos, Patsourakos, Vourlidas,..)
- Solar flares (Georgoulis, Nindos, Vlahos,..)

- The “roots” of solar magnetic activity.
- Magnetic flux emergence.
- Observations and theoretical scenario.
- Numerical approach.

Sunspots, active regions and flux emergence

Sunspots and Active Regions

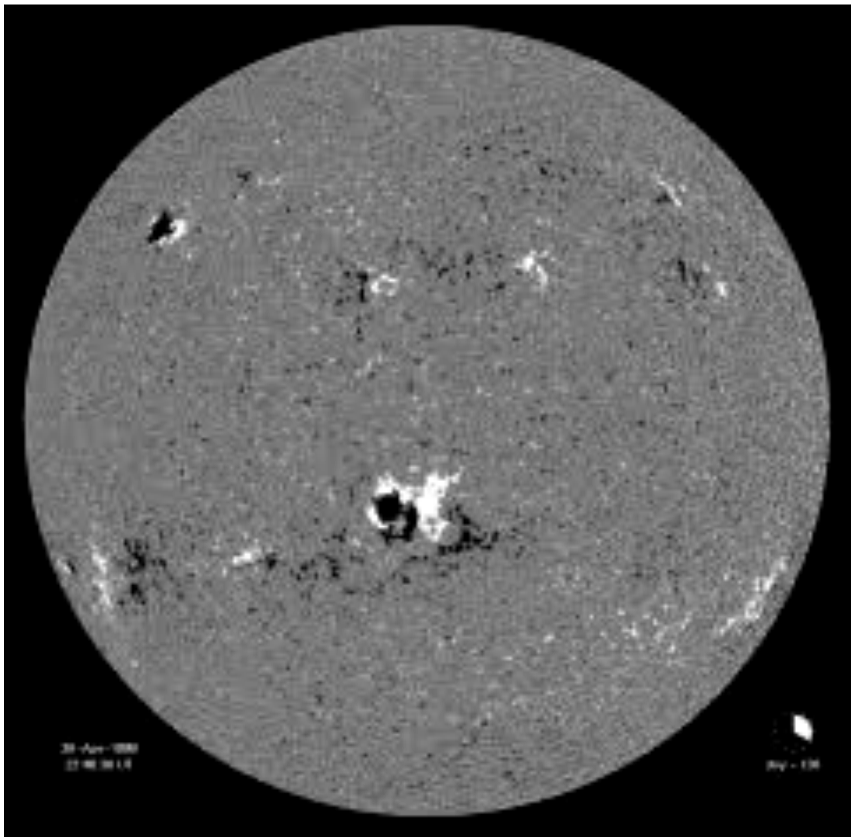

MDI, full disk magnetogram

MDI magnetogram around an Active Region

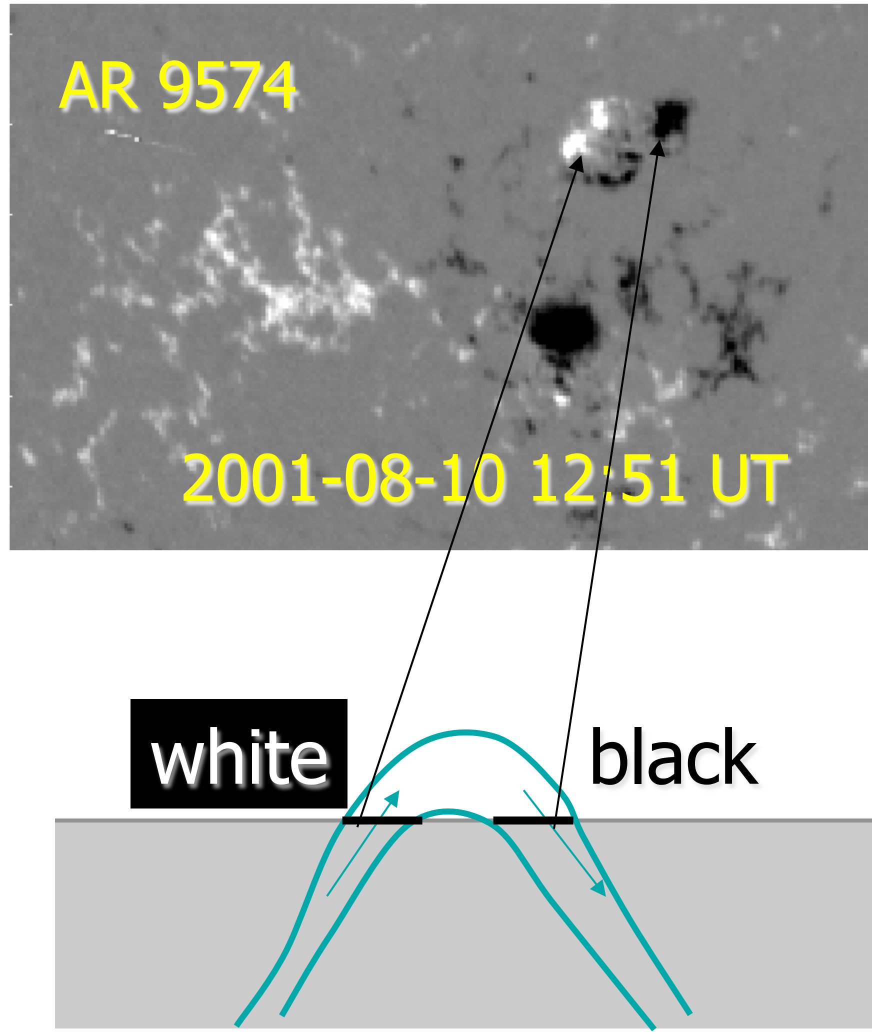

Emerging magnetic field forms sunspots

Flux emergence at the photosphere

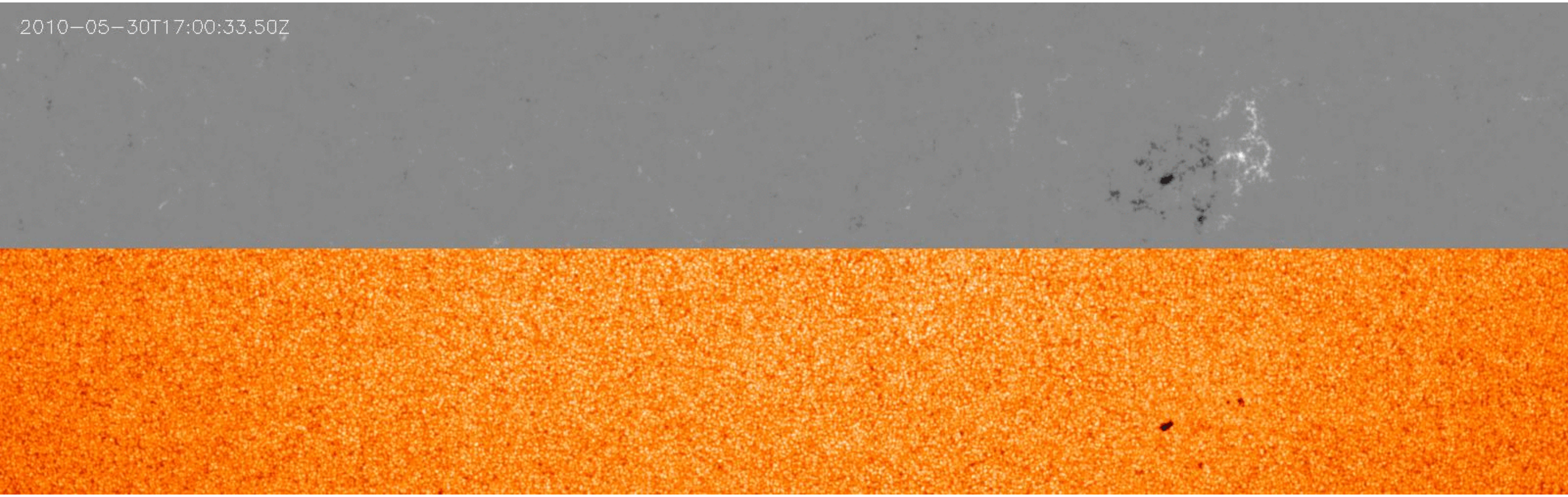

- Top: SDO/HMI magnetogram, Bottom: intensity of the continuum.
- 'Coherent' magnetic flux bundles in the two opposite polarities.
- They move apart towards an East-West direction.
- Formation of sunspots and AR 11076.

Scenario of magnetic flux emergence

Dynamo action at base of convection zone.
Magnetic buoyancy acts on the dynamo-generated magnetic field.

Total pressure continuous $P_i + (B_i)^2/2mu = P_e$
Thermal equilibrium Ti = Te
Then, since $P_i < P_e \rightarrow \rho_i < \rho_e$
B tube becomes lighter and rises (Parker 1955).

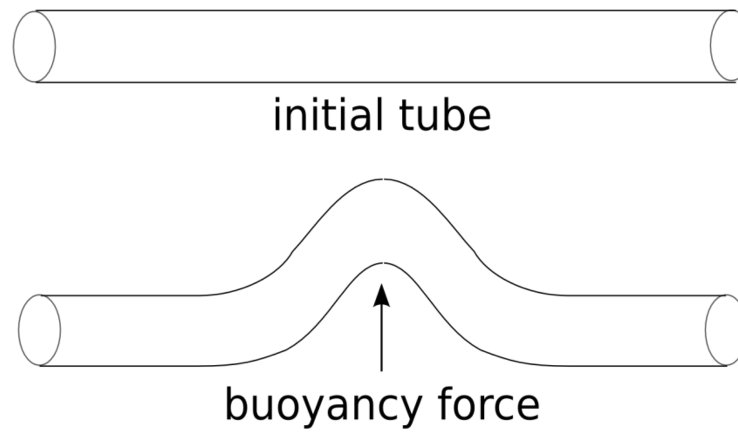

Bipolar regions appear at the photosphere (Fox, 1908).

Twisted structures apear in EFR (Strous & Zwaan, 1999 – Leka et.al, 1996).

Formation of W-loops and arch filament systems (Bruzek, 1967).

Observations of eruptive phenomena, flares, CME's due to flux emergence (Chifor et. al, 2006, Dun et.al 2007, etc.).

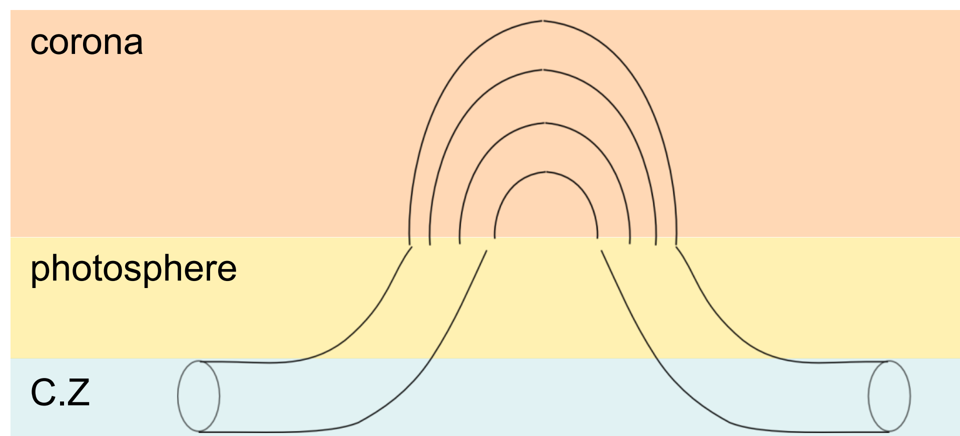

Initial conditions: atmosphere and magnetic field

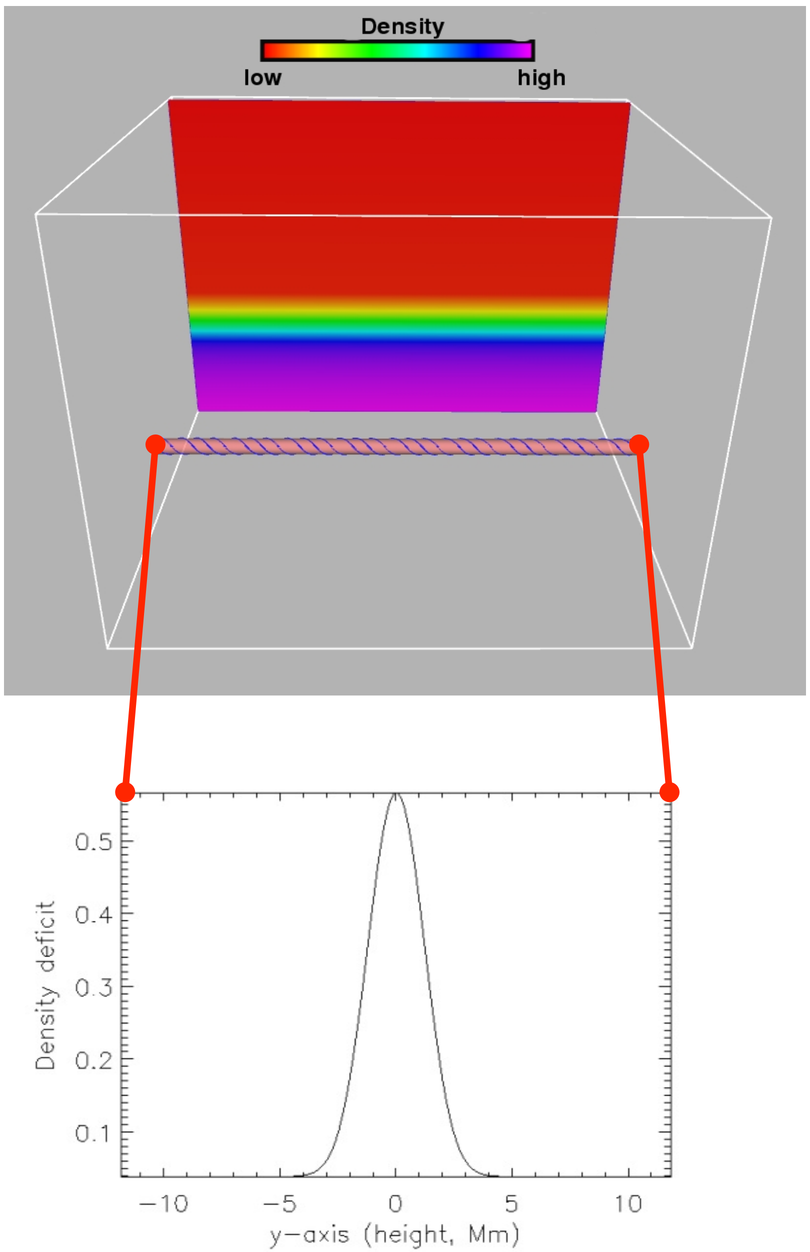

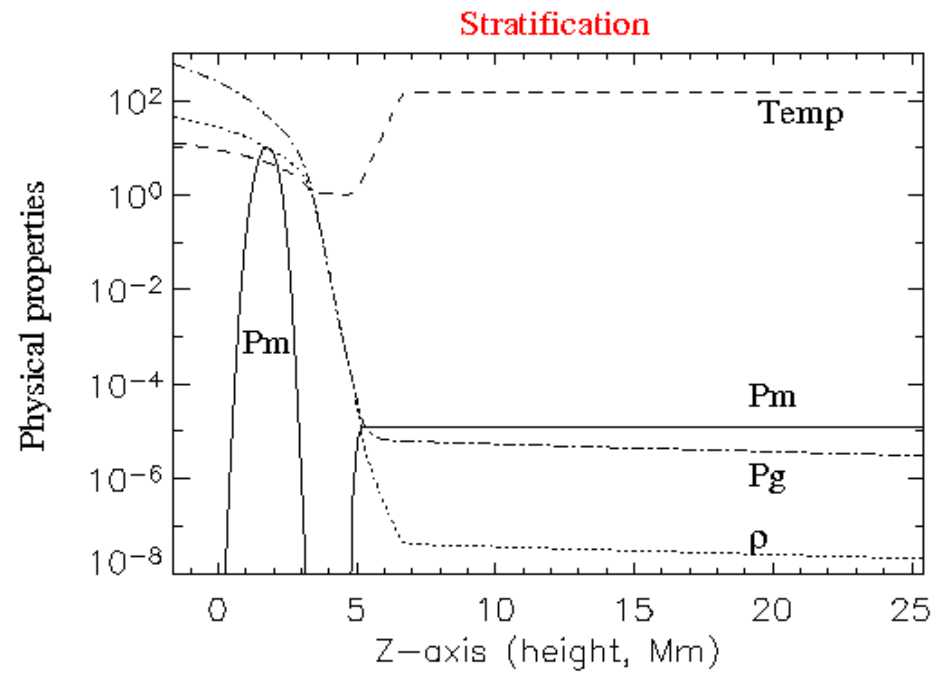

$B_y = B_o \cdot e^{(-r^2/R^2)}$ - $R = 425$ km

$B_\phi = a \cdot r \cdot B_y$, $a = 0.4$

$\rho(x,y,z) = (P(x,y,z)/P_{st}) \cdot \rho st(z) \cdot e^{(-y^2/\lambda^2)}$ - $\lambda = 3$ Mm

$B_o = 3.8$ kG, $\beta = 12.8$

$B_c = B_c(z)(\cos(\phi), \sin(\phi), 0)$, $B_{cor} = 13$G, $\beta = 0.06$

Numerical method

Three dimensional time-dependent resistive MHD equations

$$
\begin{aligned}
\frac{\partial \rho}{\partial t} &= -\nabla \cdot (\rho \mathbf{u}), \\
\frac{\partial (\rho \mathbf{u})}{\partial t} &= -\nabla \cdot (\rho\, \mathbf{u} \otimes \mathbf{u} + \underline{\underline{\tau}}) - \nabla p + \rho\, \mathbf{g} + \mathbf{J} \times \mathbf{B}, \\
\frac{\partial e}{\partial t} &= -\nabla \cdot (e \mathbf{u}) - p\, \nabla \cdot \mathbf{u} + Q_{\mathrm{Joule}} + Q_{\mathrm{visc}}, \\
\frac{\partial \mathbf{B}}{\partial t} &= -\nabla \times \mathbf{E}, \\
\mathbf{E} &= -(\mathbf{u} \times \mathbf{B}) + \eta \mathbf{J}, \\
\mathbf{J} &= \nabla \times \mathbf{B}, \\
p &= \rho T \frac{\mathcal{R}}{\tilde{\mu}},
\end{aligned}
$$

Copenhagen Stagger Code

+

Lare3D code

· 6th order - partial derivatives
· 5th order - interpolation
· 3rd order - predictor-corrector - time stepping
· Stretched staggered grid 1d, 3d
· Periodic and closed BC
· Damping zone top-bottom
. Hyperdiffusive scheme, 4th order quenced diffusion operators

Related work

- Magara, et.al, 2001, ApJ., 549,608
- Fan, Y., 2001, ApJ., 554,111
- Abbett,W.P., Fisher, G.H., 2003, ApJ.,582,475
- Magara,T., Longcope,D., 2003, ApJ., 586,630
- Manchester et.al 2004, ApJ, 610, 588
- Gibson, S.E. & Fan, Y.,111, JGR 2006
- Murray, et al 2006, A&A, 460, 900
- MacTaggart, D., Hood, A., 2010, ApJ, 716, 219

Idealized simulations

……………………….

- Leake, J.E & Arber, T.D., 2006, A&A (*partial ionization*).
- Abbett, W.P, 2007, ApJ (*conv. + rad. losses + strong stratification*).
- Cheung, M. et.al, 2007, A&A (*conv. + radiative transfer*).
- Martinez-Sykora, J. et.al, 2008, ApJ (*conv. + radiative transfer + thermal conduction + strong stratification*).
- Tortosa, A. & Moreno-Insertis, F. 2009, A&A *(conv/phot/chrom + rad transfer).*
- Cheung, M. et.al., 2010, ApJ *(conv/phot. + radiative transfer*).
- Stein, R. et.al, 2011, Solar Physics (*deep conv/phot. + rad.transf.*)

Realistic simulations

…………………………..

- Emergence in the photosphere.
- Magnetic ‘tails’.
- ‘Sea-serpent’ configuration.
- Unloading of mass.

Initial phase: emergence in the photosphere

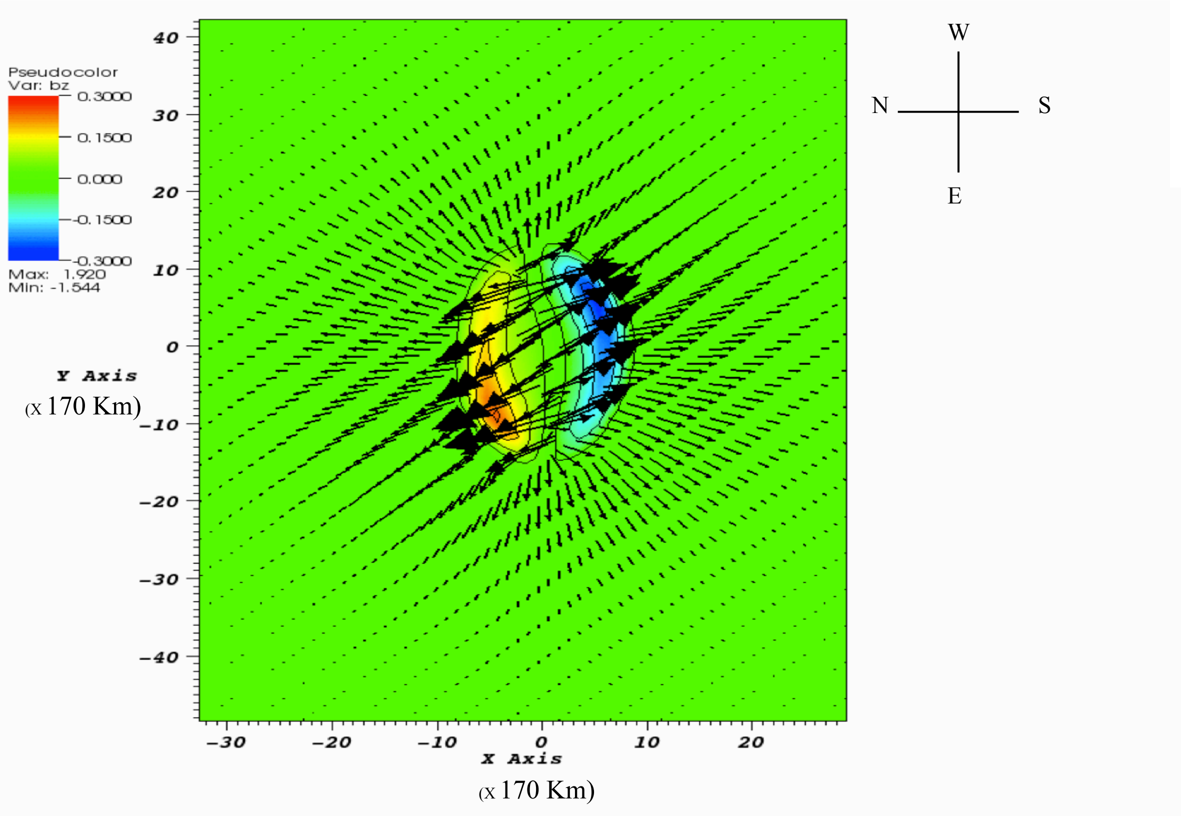

- Density deficit & buoyancy effect: tube rises to the photosphere.

- V_{rise}=1.7 km/sec, t=12.5 min.

- Formation of a bipolar region.

- B ~ 600G at the photosphere.

- Formation of 'tails' on both sides of PIL.
- Location of sunspot formation.
- Organized shear velocity flow in the photospheric layer.
- Inflow in the transverse direction.

Related work: Fan (2001), Manchester (2004), etc.

Flux emergence, NOAA AR 10808

Observations

Simulations

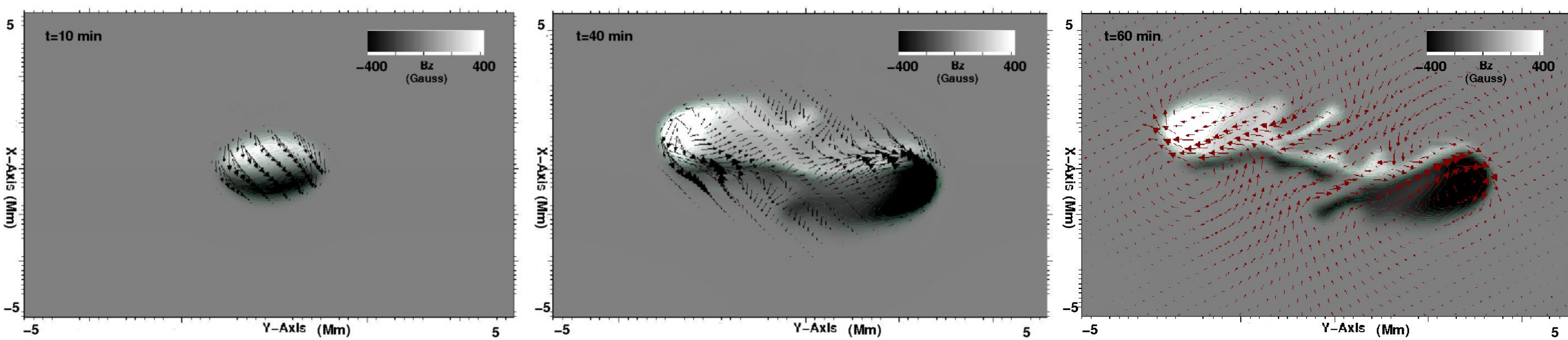

Magnetic 'tails': *a twisted flux tube is emerging from below* (*Archontis & Hood, A&A (2010)*).

Related work: Lopez Fuentes, M.C. et.al ApJ (2000), Canou, et.al ApjL (2009)

Complex, multi-scale flux emergence

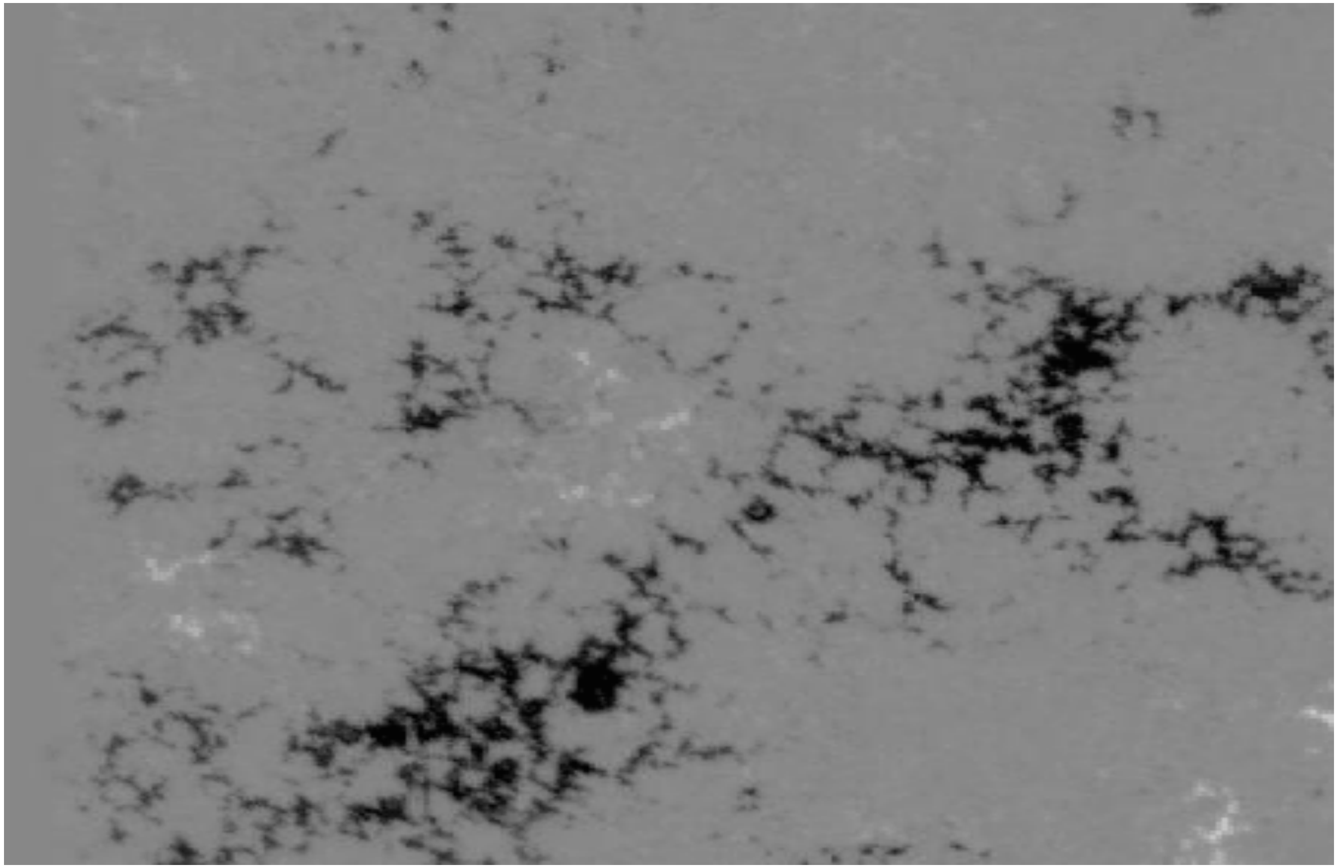

‘Complex’ emergence of magnetic flux on small-scales and formation of a large-scale AR.

Hinode/SOT, December 1-2 (2006)

Related work: Magara, T. ApJ, (2008), Harra, L. et.al, Sol.Phys, (2010), Del Zanna, G. et.al A&A, (2011)

The development of ‘sea-serpent’ fieldlines

Interaction with convective flows

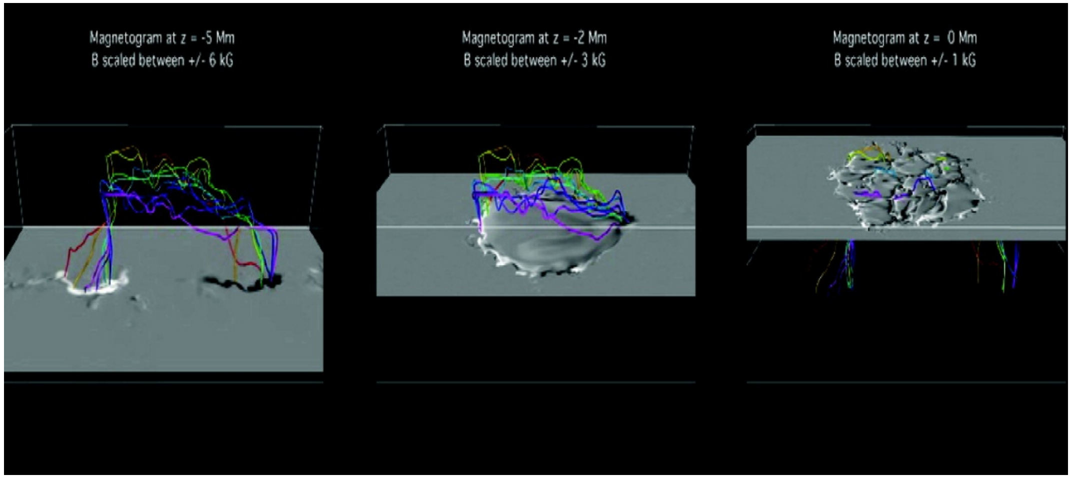

Cheung, et al ApJ, 687 (2008)

Parker instability in flux tubes

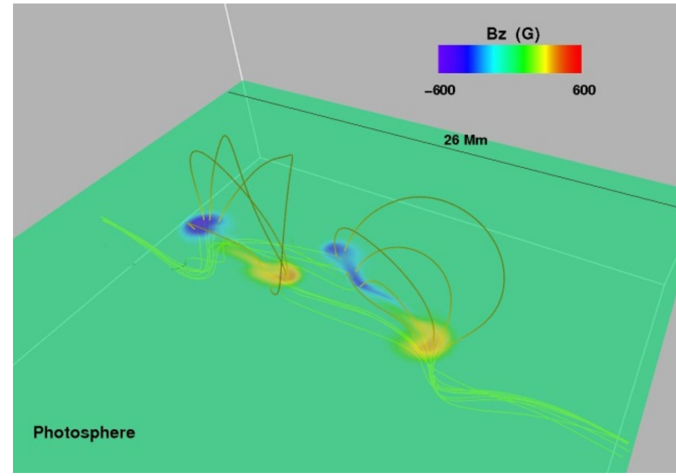

Archontis & Hood, A&A, 514 (2010)

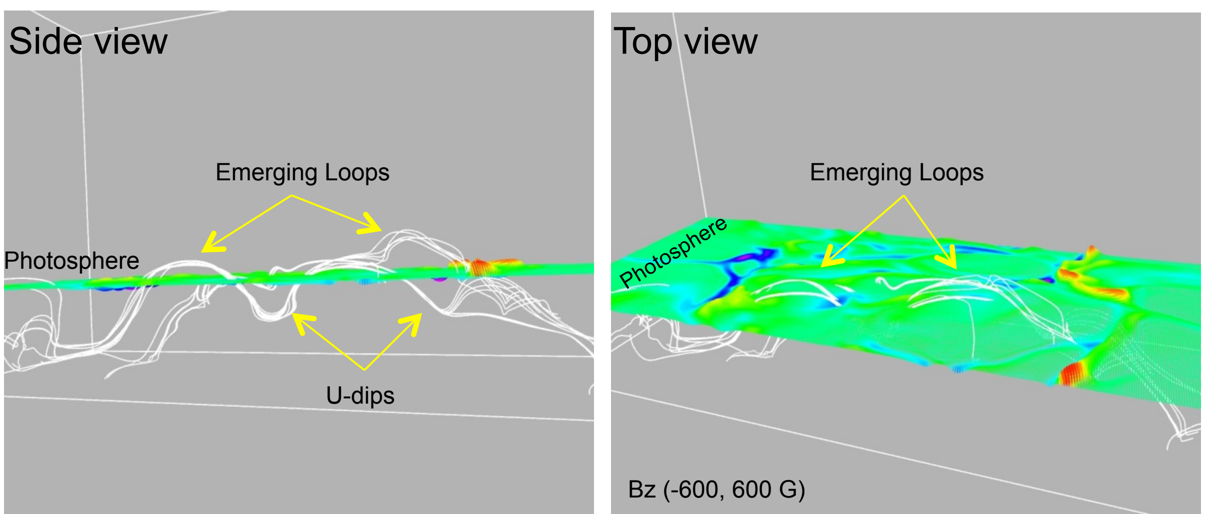

Parker instability in flux sheets

Archontis & Hood, A&A, 508 (2009)

Photosperic and coronal response

Ha 0.8 Å , Filtergram of AR8844

Flare Genesis Experiment

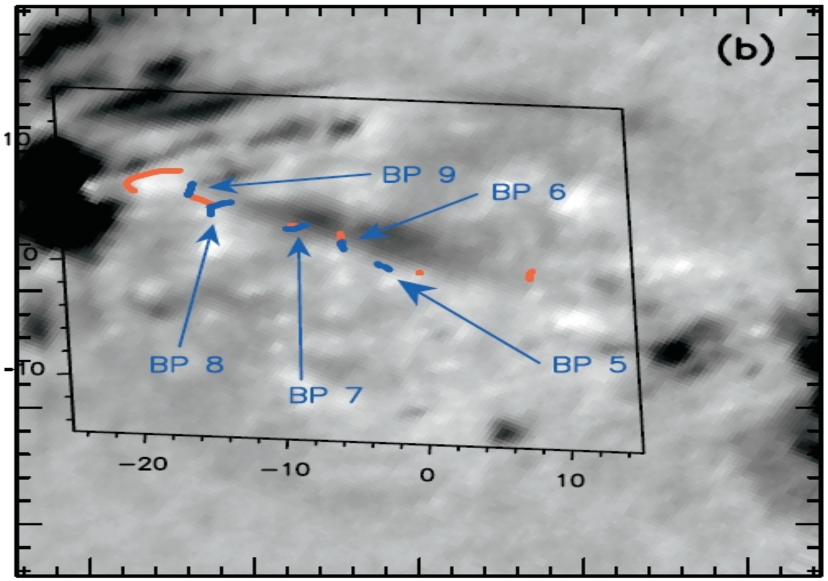

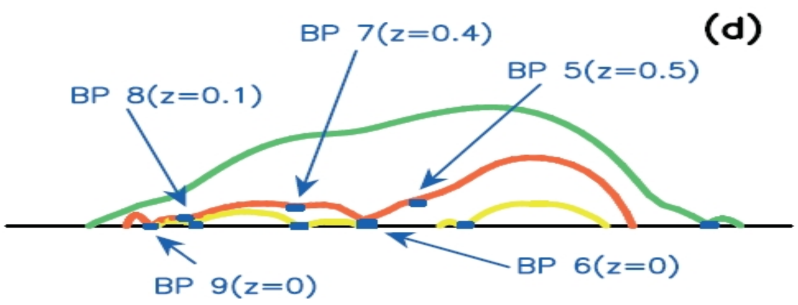

Pariat et.al, ApJ (2004)

Theoretical interpretation

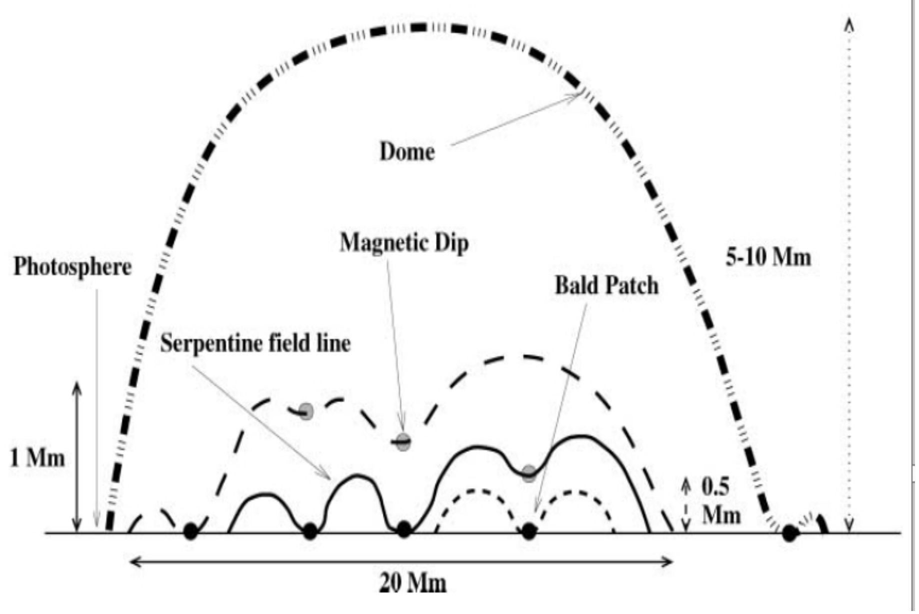

Emergence of a 'sea-serpent' magnetic field via successive reconnection events.

Related work: Chen, et.al (2001),
Georgoulis et.al (2002),
Matsumoto et.al (2008), etc.

‘Sea-serpent’ emergence – 2.5D and 3D experiments

Isobe, Tripathi & Archontis, ApJL (2007)) - 2.5D

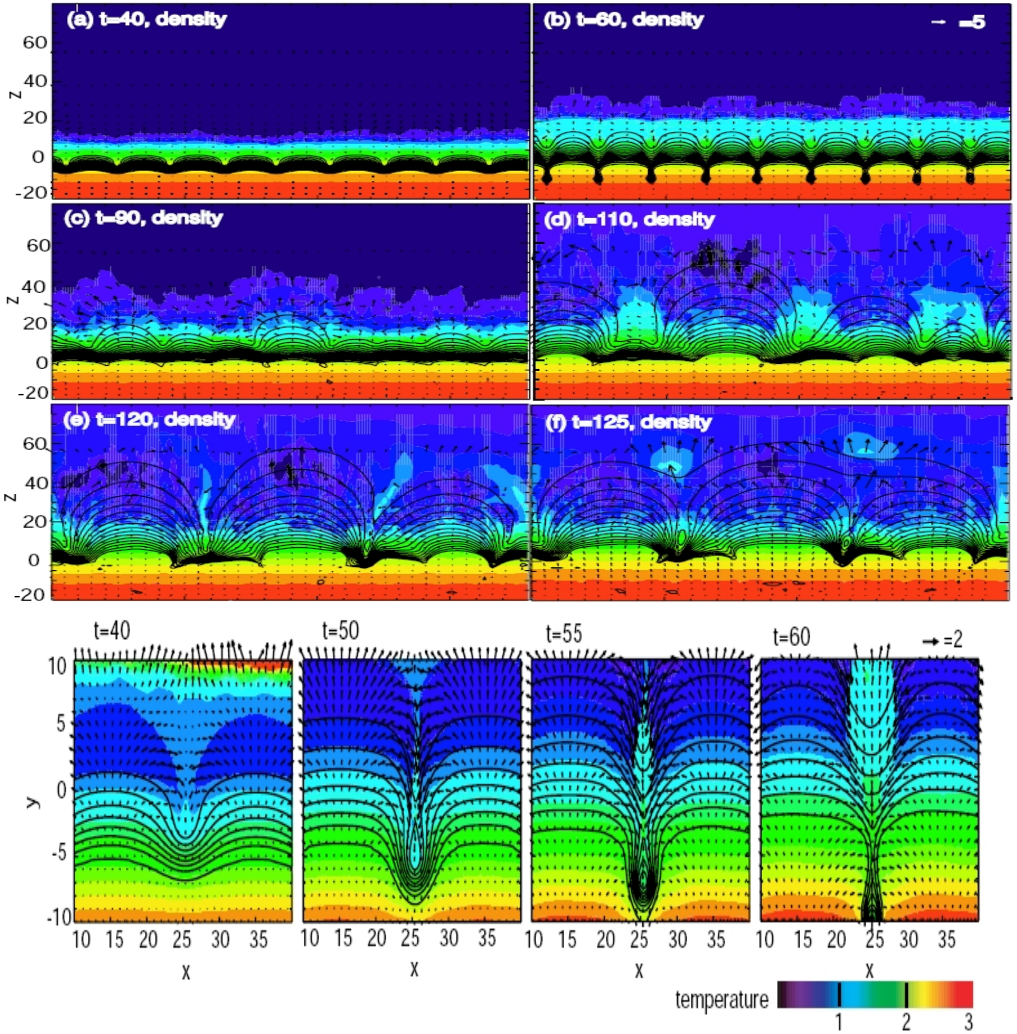

Archontis & Hood , A&A 508, (2009) - 3D

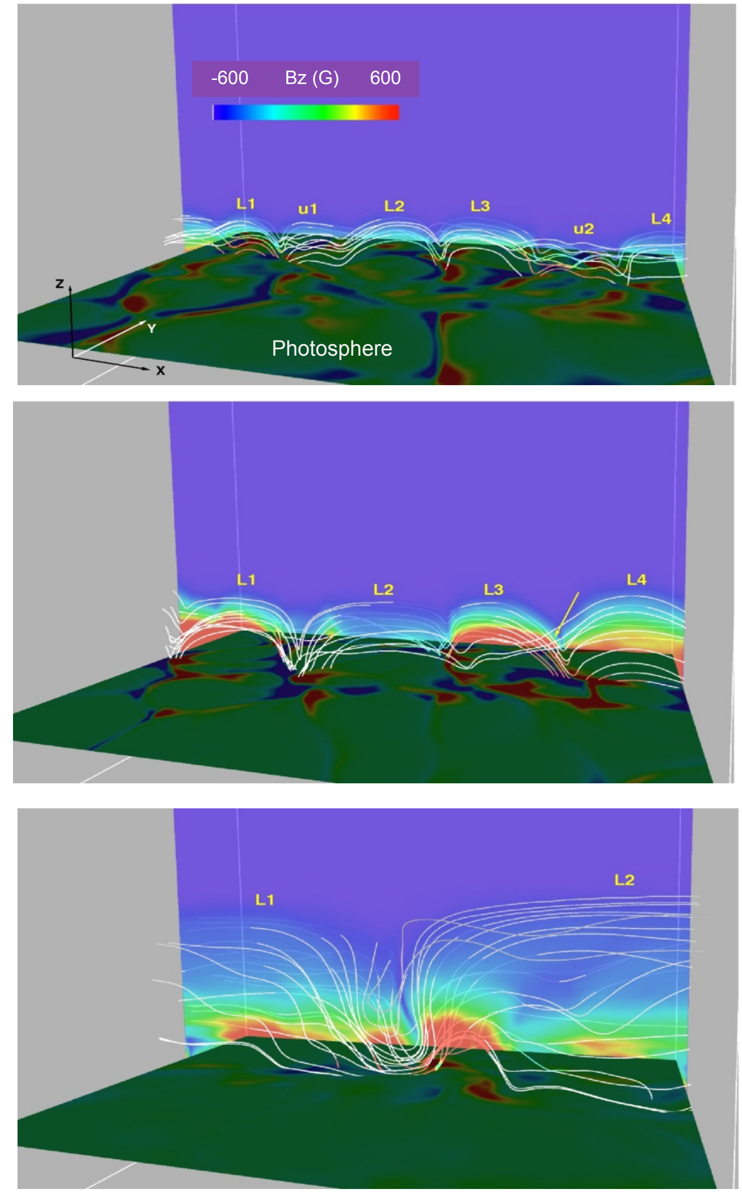

Ellerman Bombs?

Agreement with results by Kitai, R (1983), etc.

The unloading of mass – a robust generic result?

Tortosa, A. & Moreno-Insertis, F. A&A 507, (2010)

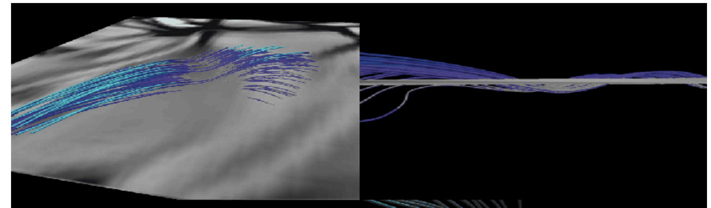

Archontis & Hood A&A 508, (2009)

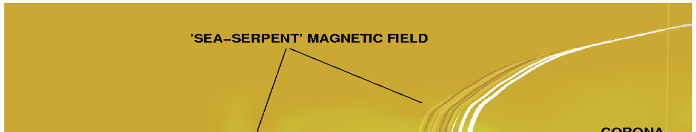

Progress is only possible through the interplay of:

- idealized numerical experiments

- realistic numerical simulations

- observations from all atmospheric layers

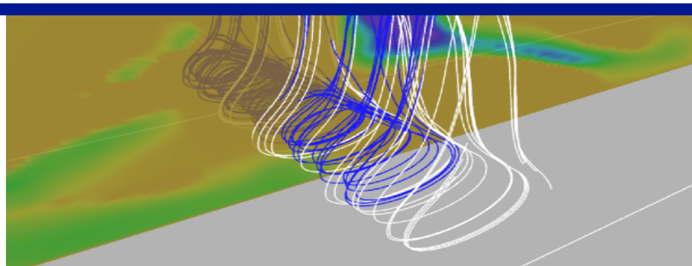

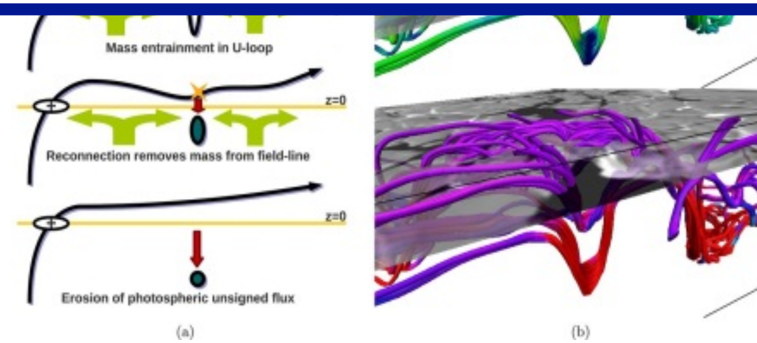

- Large-scale evolution of the field.
- Twisted flux tube models.
- Coronal flux ropes.
- Sigmoids, jets, plasmoids, heating.

3D topology and shearing of the field

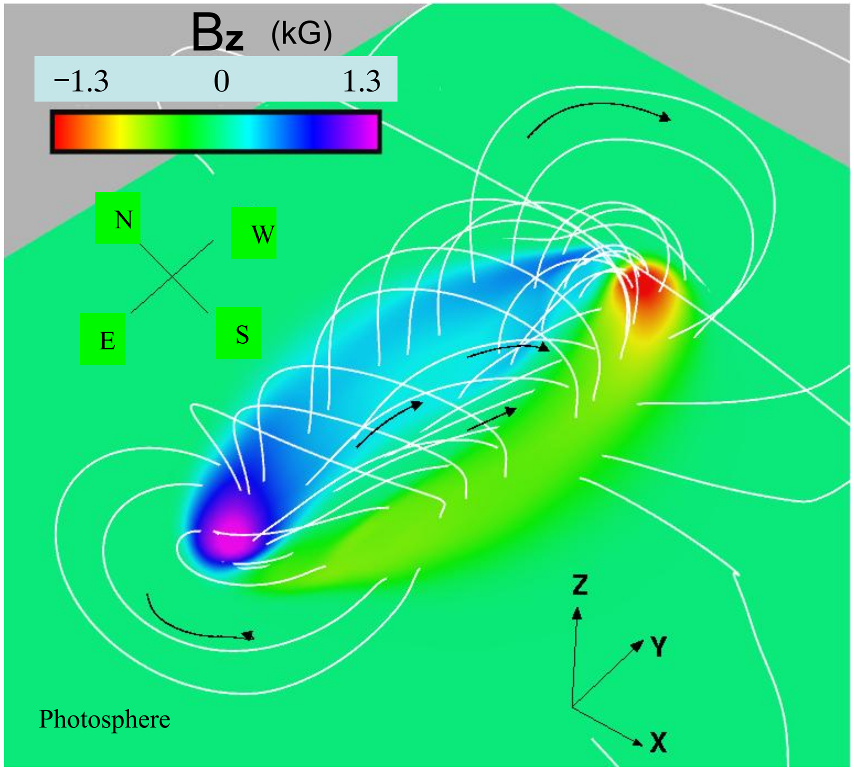

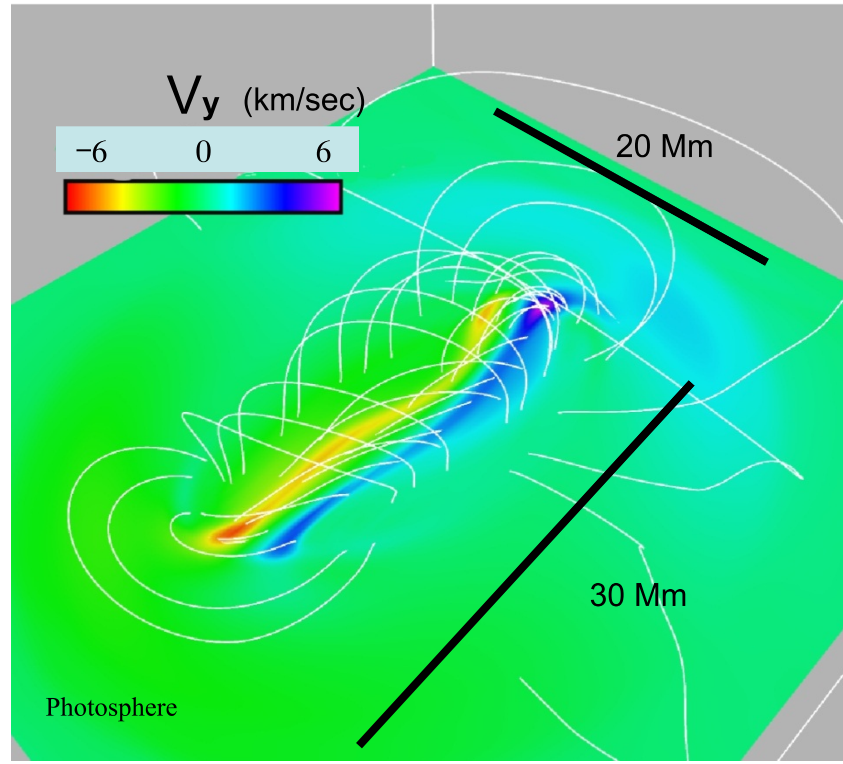

- Inner fieldlines are lying mostly along the neutral line.
- Outer fieldlines have a strongly azimuthal nature.
- Shearing of the field occurs along the neutral line but also along height.

- As the two polarities are moving in opposite directions along the neutral line, the shear flow can reach up to 10 km/sec.

Archontis et.al, ApJ , 691 (2009)

van Ballegooijen and Martens (1989)

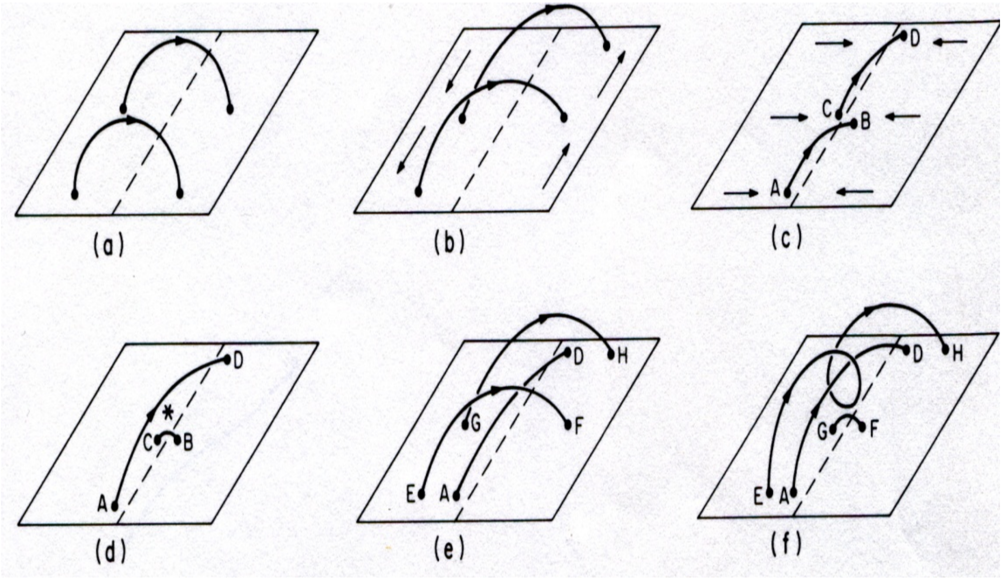

shearing motion + convergence + reconnection

current sheets, longer loops and helical magnetic field structures that rise higher into the atmosphere.

‘New’ magnetic flux ropes

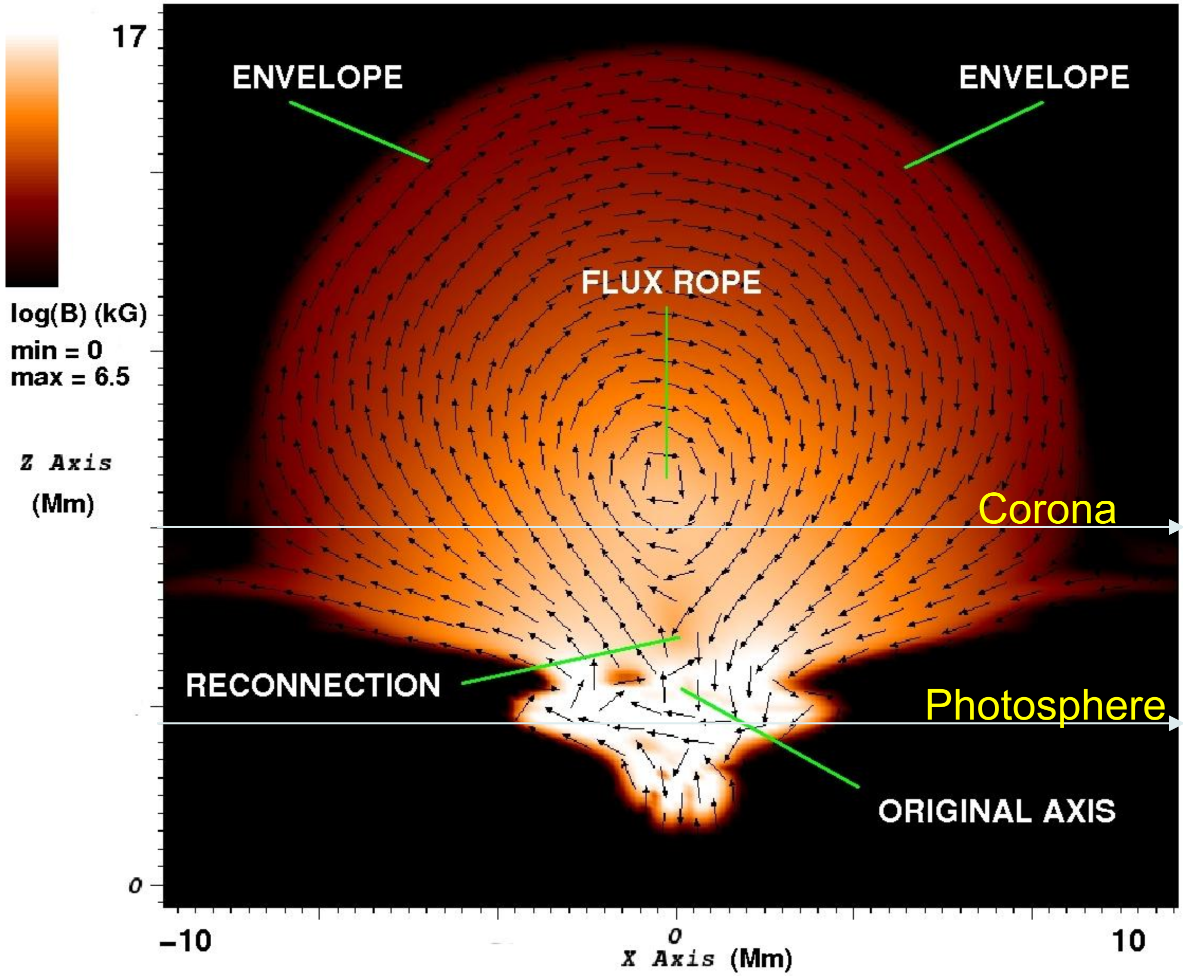

- The new rope is formed via internal reconnection.
- The expansion forms an envelope magnetic field.
- The original axis stays at photosphere.
- The new flux rope rises into the corona.
- The envelope field surrounds the new rope.

(In)stability /eruption of flux ropes: Demoulin & Aulanier, ApJ, 718 (2010), Torok & Kliem, ApJ, 630 (2005)

Failed expulsion of magnetized plasma

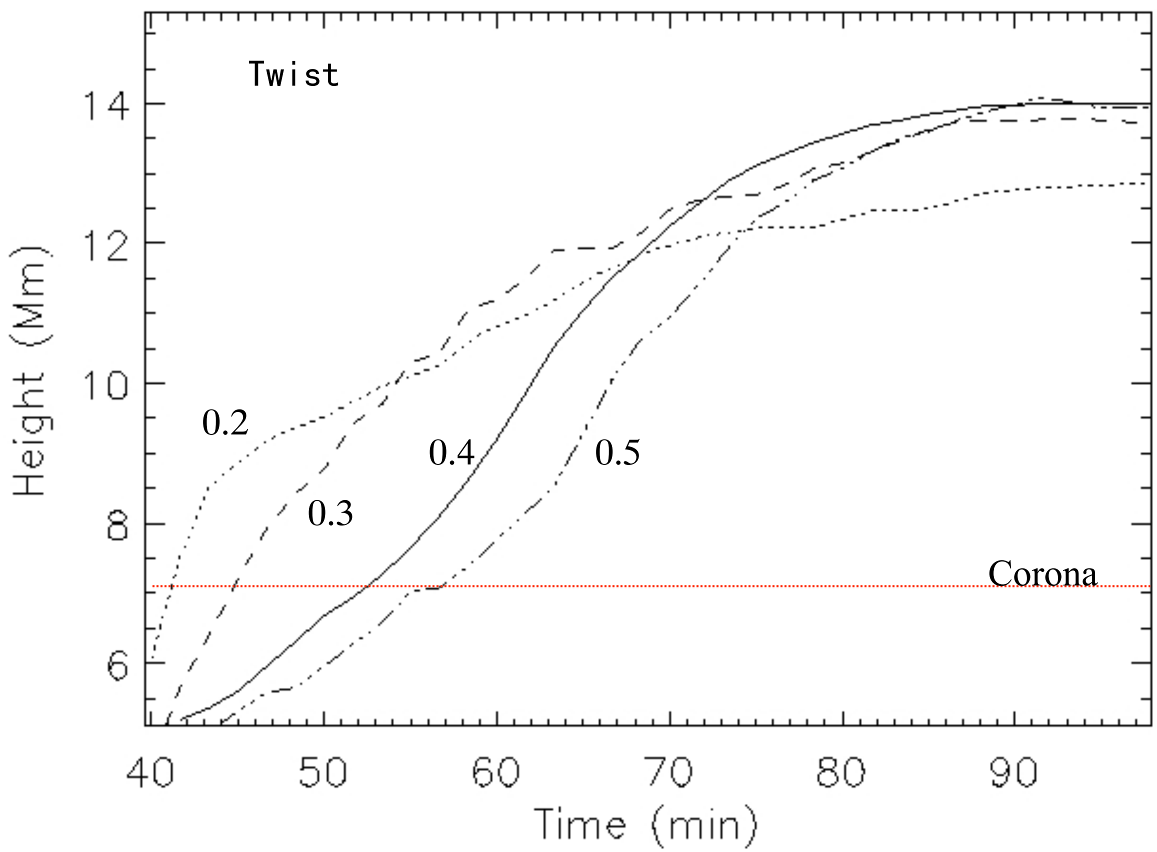

- The new rope *fails* to emerge into the high corona.
- No break-out.
- Small twist: early eruption.
- Strong twist: two phases.
- End: Quasi-static equilibrium.

Related work: Archontis & Torok A&A, 492 (2008) , Archontis & Hood A&A (2011, submitted)

Emergence of dense magnetized plasma

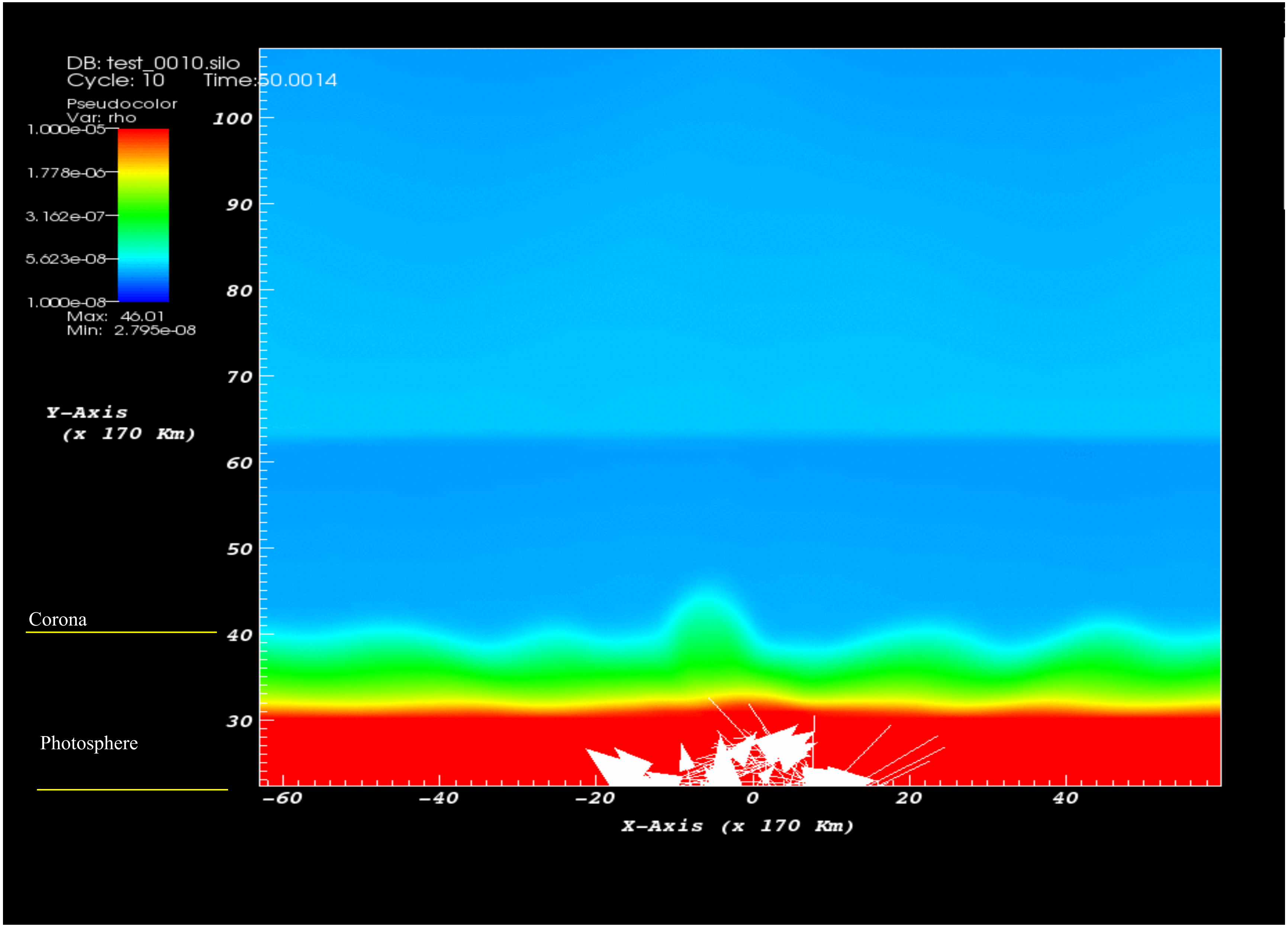

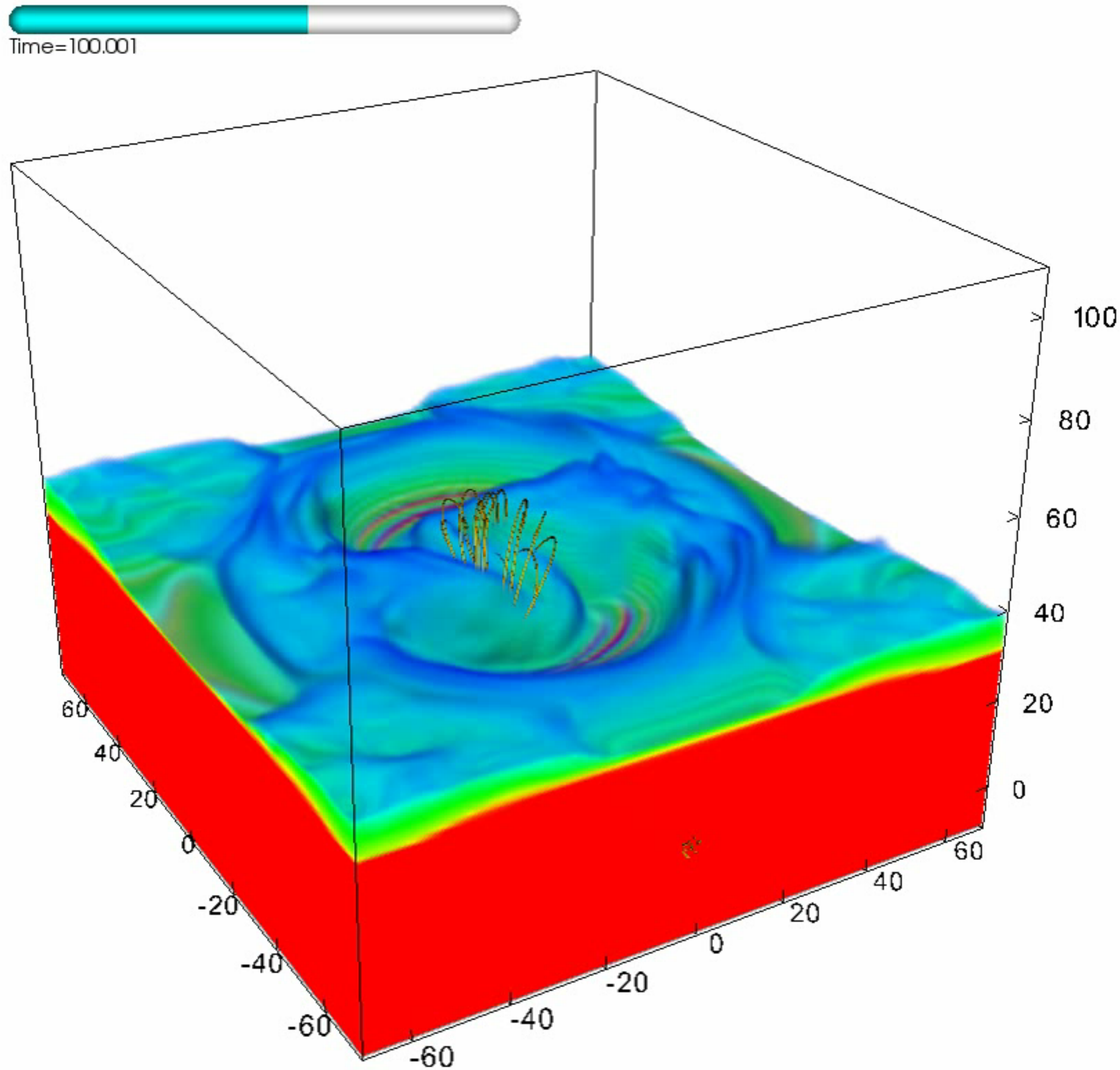

Time=100.001
100
80
60
40
20
0
60
40
20
0
-20
-40
-60
-60
-40
-20
0
20
40
60

Sigmoids in the Sun

Hinode – XRT, coronal sigmoid

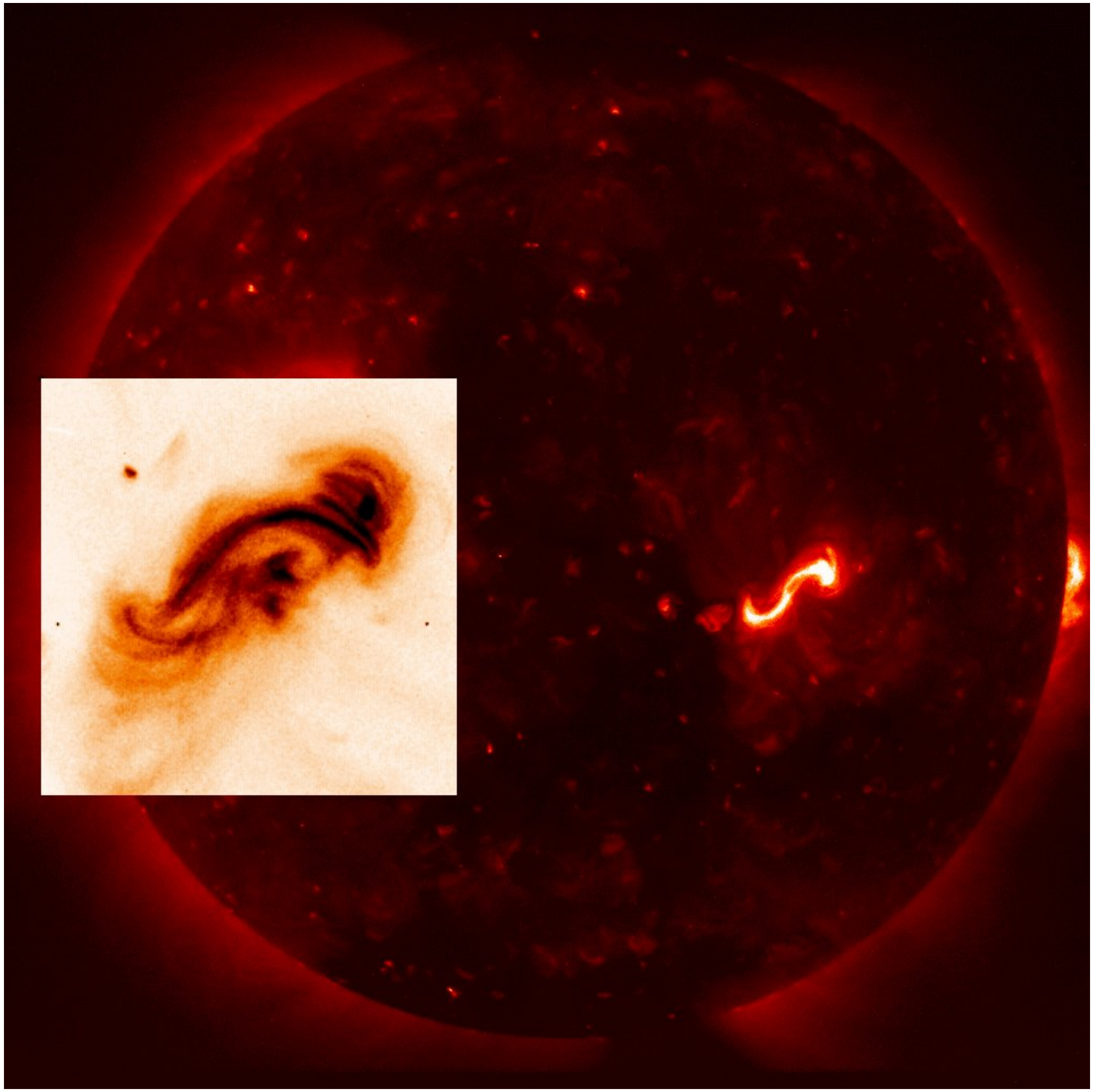

Eruption of sigmoid, 12 Feb. 2007

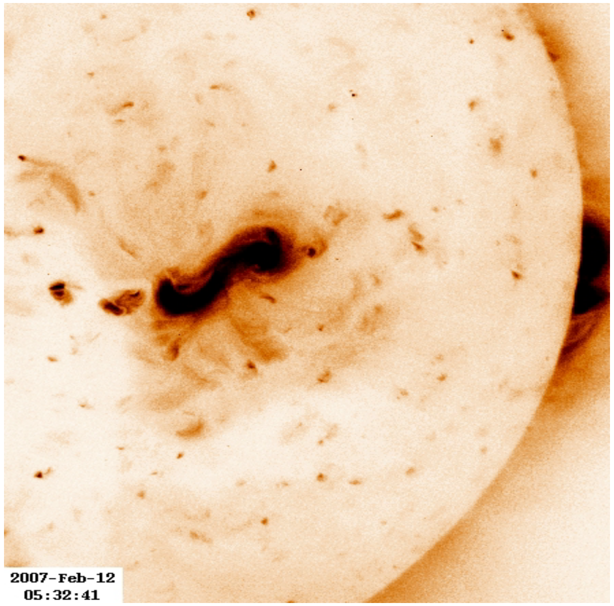

Related work: MacKenzie & Canfield A&A (2008)

Sigmoids: a flux emergence model

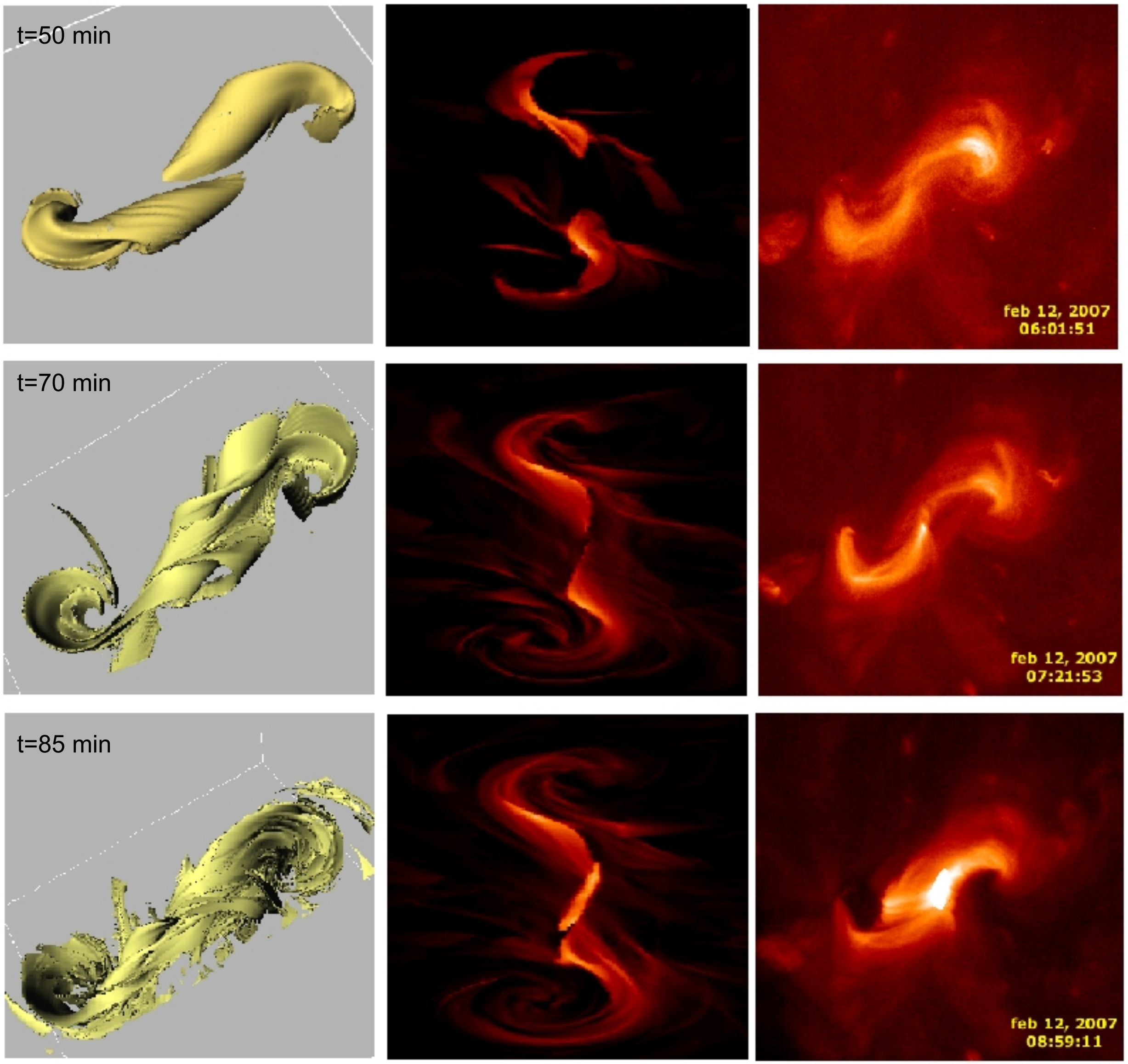

| J | $\int J^2\, dz$ 0.6<T<2.5 MK   XRT

- Sigmoids observed in X-Rays.
- Main features (MacKenzie & Canfield, 2008)
- Initial 2 J-like structures (Titov & Demoulin, 1999)
- Many threads to form S-like structure in (**jxB**/B)
- ‘Flaring’ in the middle of sigmoid and eruption of coronal flux rope.

XRT images provided by Savcheva, A & Golub,L, SAO.

Related work: Archontis,et.al ApJ (2009)

Emergence into an overlying coronal magnetic field

$\Phi \approx 180$ deg. ‘antiparallel’ fieldlines

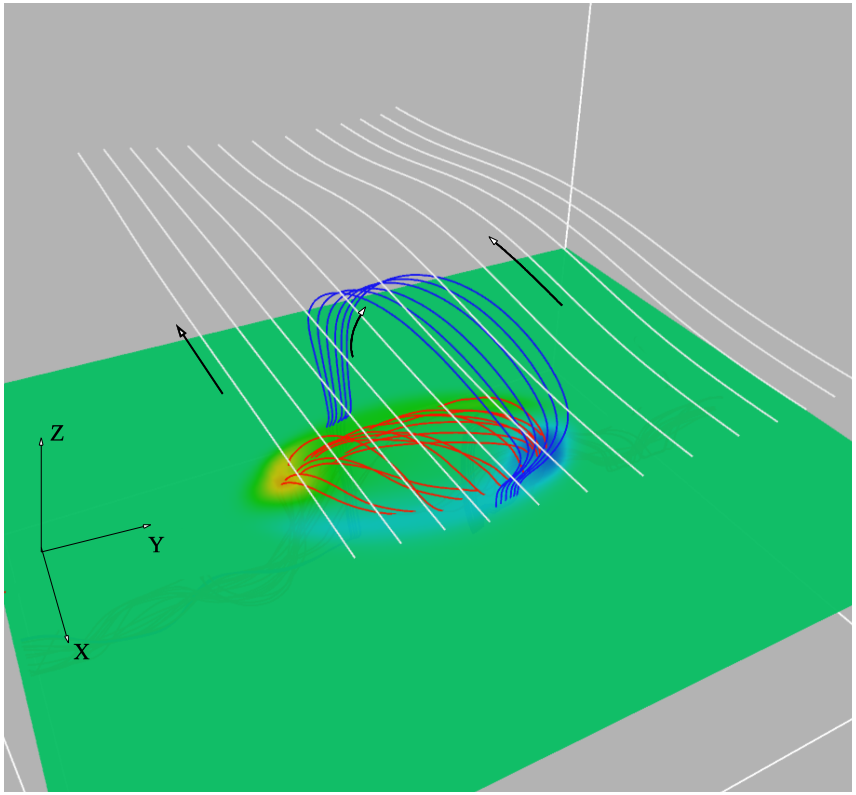

$\Phi \approx 90$ deg. ‘perpendicular’ fieldlines

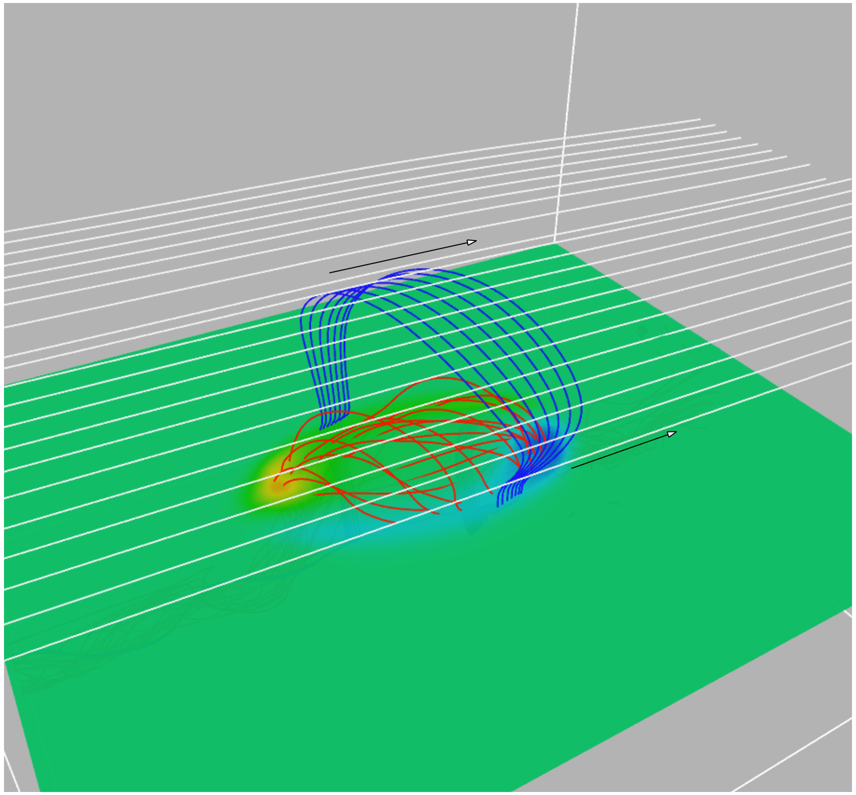

Φ is the relative contact angle.

Emerging fieldlines (blue, red), coronal fieldlines (white).

Related work: Galsgaard, et.al ApJ V666, I1 (2007)

Successful expulsion of magnetized plasma

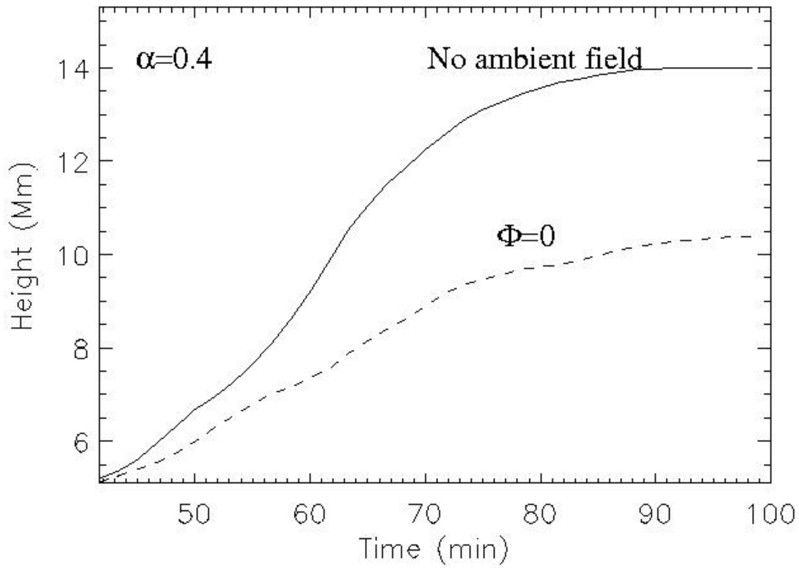

No external reconnection

- Φ=0 (‘parallel’ ambient field).
- *Failed* or *confined* expulsions.
- Weak ambient, larger expulsion heights.

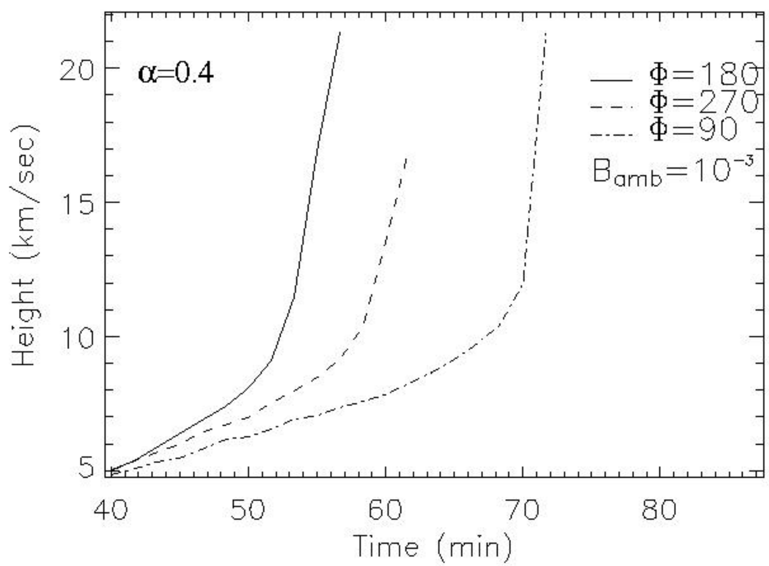

Efficient reconnection

- *Successful* expulsions.
- Remove envelope tension.
- More efficient, earlier eruption.
- Deformation, annihilation.

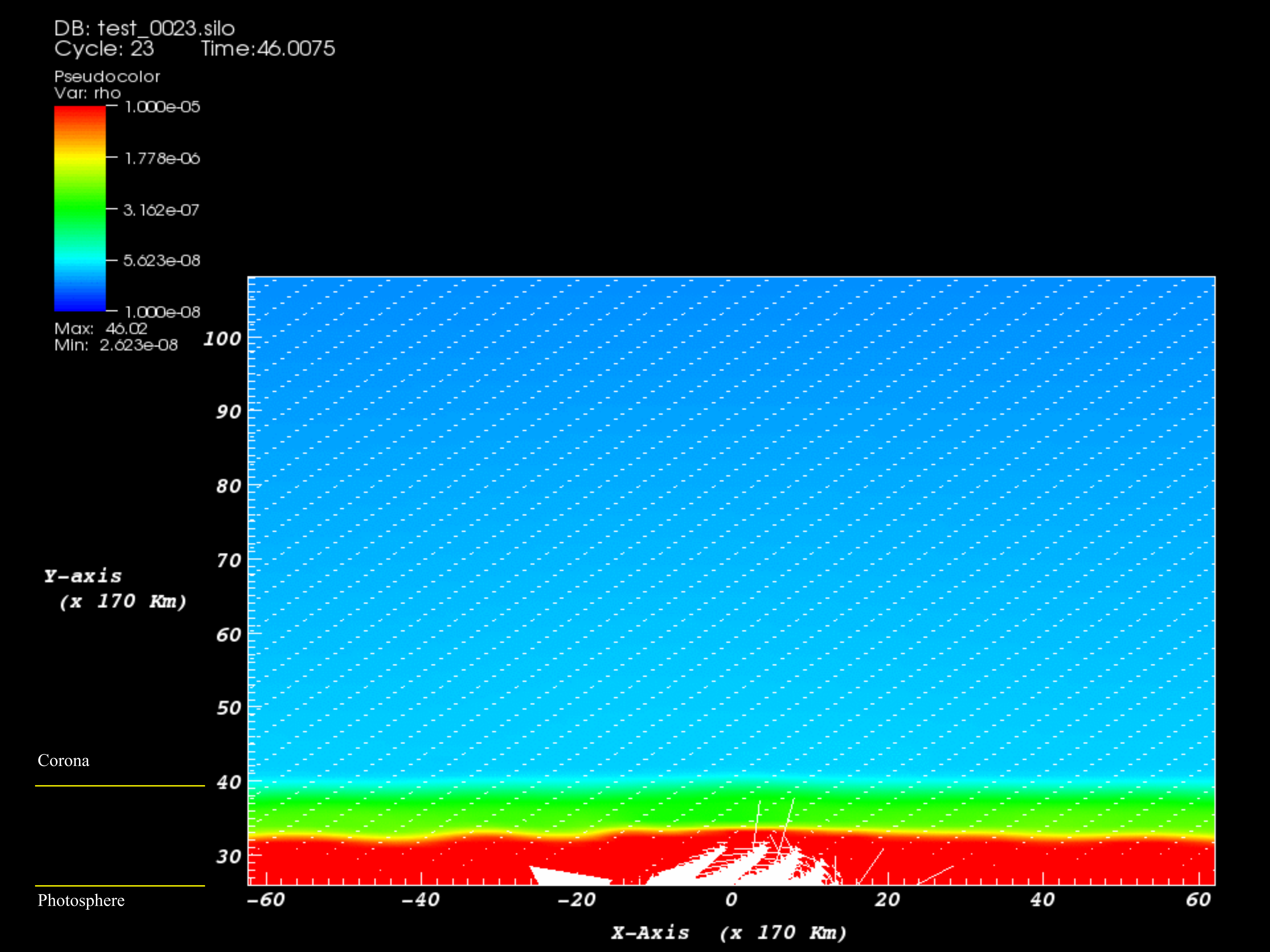
DB: test_0023.silo
Cycle: 23 Time:46.0075
Pseudocolor
Var: rho
1.000e-05
1.778e-06
3.162e-07
5.623e-08
1.000e-08
Max: 46.02
Min: 2.623e-08
Y-axis
(x 170 Km)
100
90
80
70
60
50
40
30
Corona
Photosphere
-60
-40
-20
0
20
40
60
X-Axis (x 170 Km)

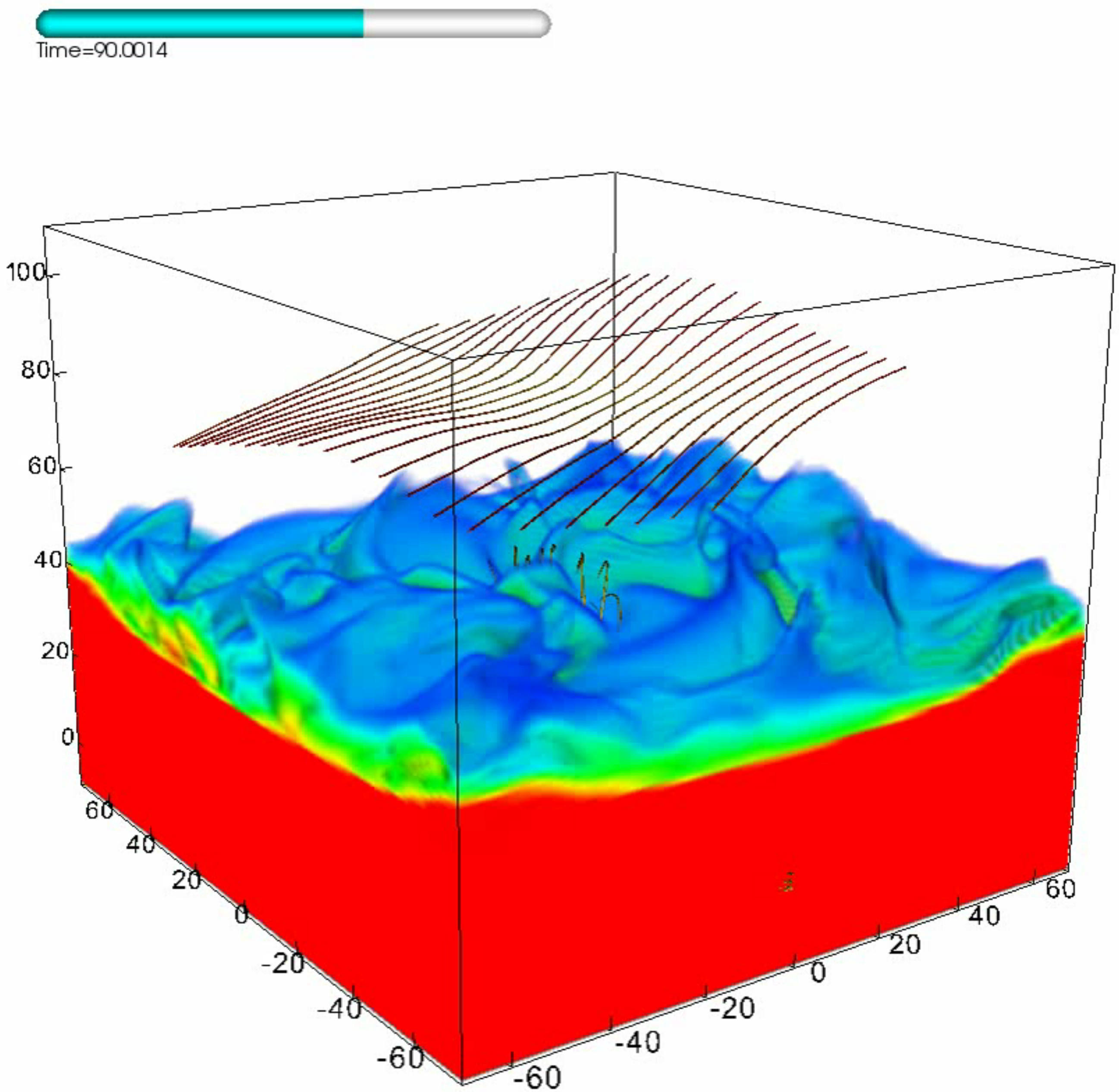

Time=90.0014
100
80
60
40
20
0
60
40
20
0
-20
-40
-60
60
40
20
0
-20
-40
-60

Run-away rising motion of dense plasma

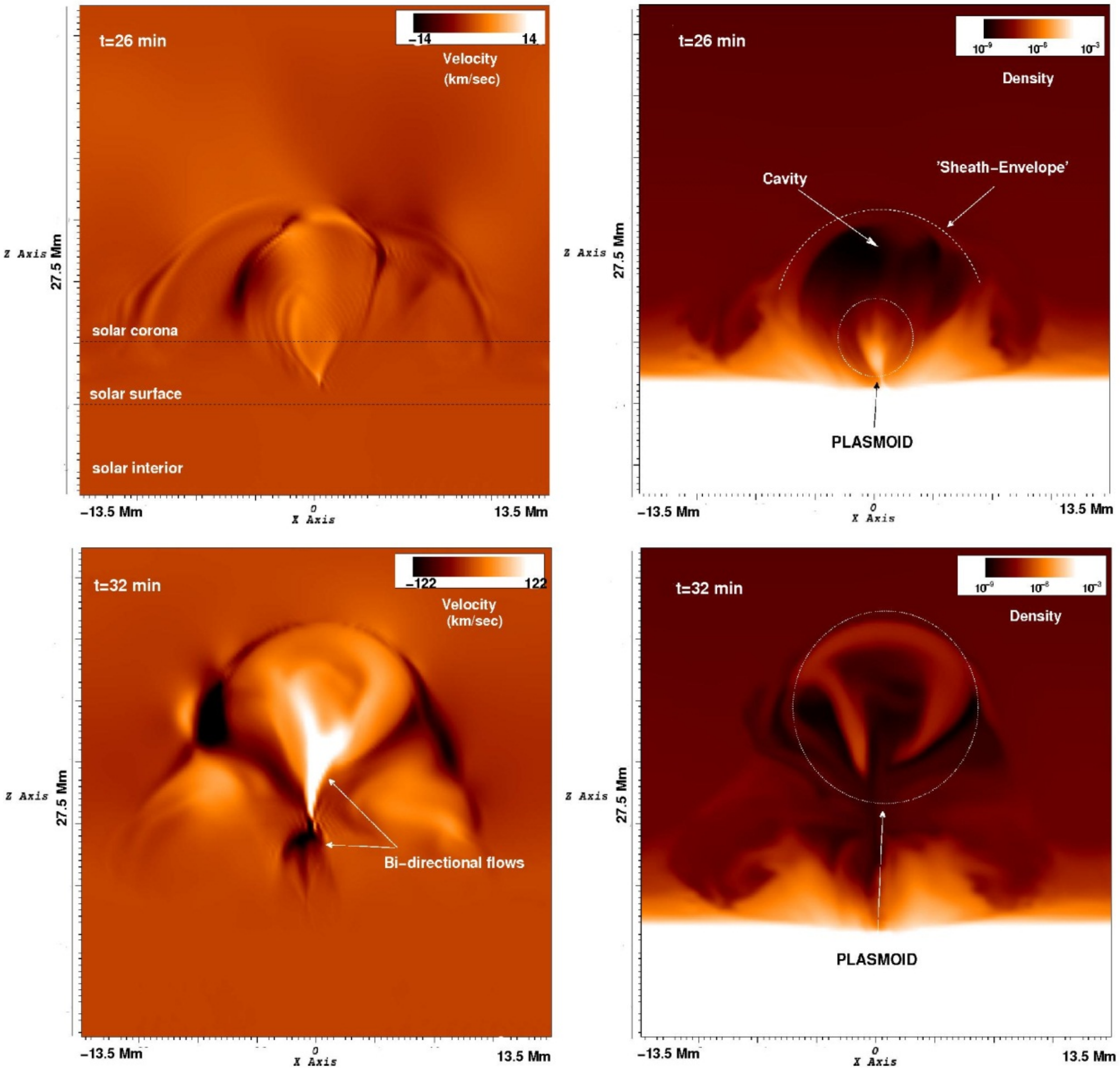

- Φ=90, Vz(left), density(right).
- Upflows, front and tail.
- Profound downflows.
- Two different magnetic systems.
- Cavity-like configuration.
- Dense coronal erupting plasma.
- Draining of plasma.
- Heavier: 1-2 orders of magnitude.

Archontis & Hood (2011, A&A submitted)

How fast are these expulsions ?

Magnetic flux rope

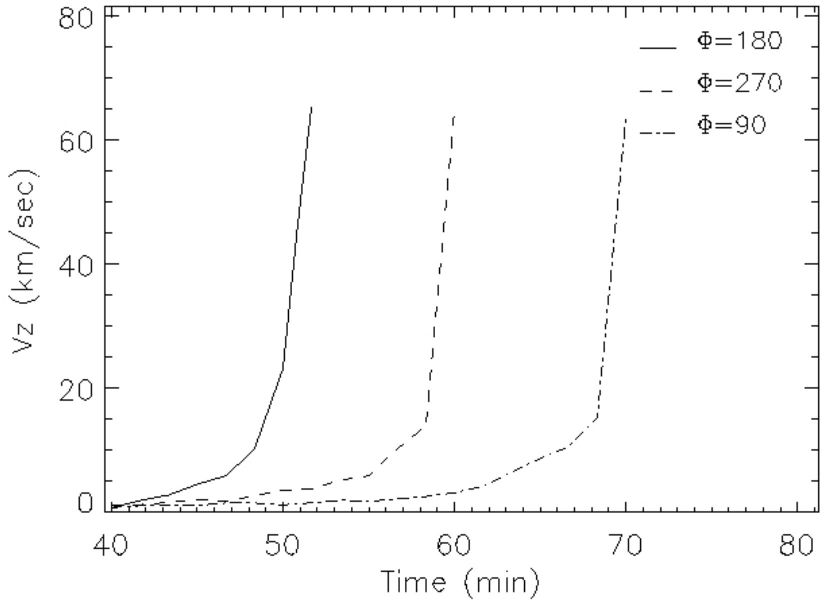

Reconnection jet

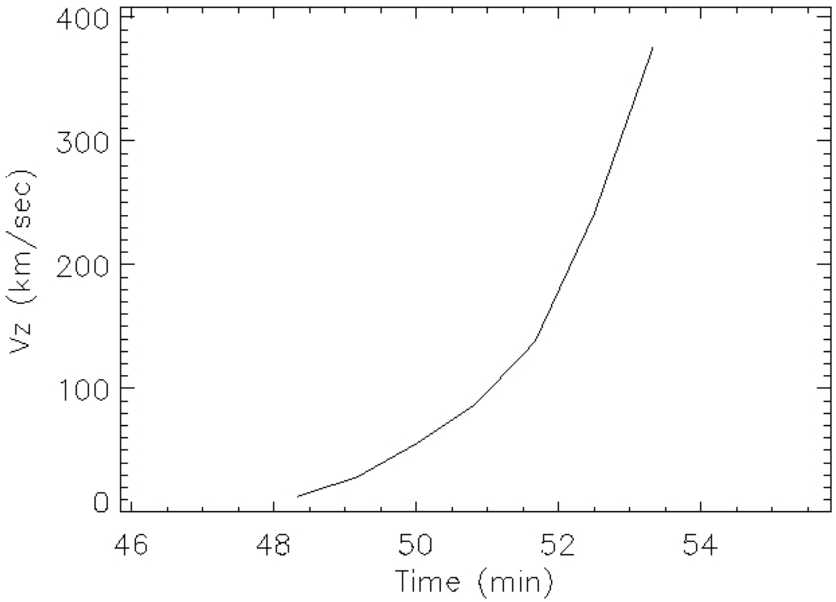

- Two phases: slow-rise, fast-rise.
- Rope center: max speed 60-70 km/sec.
- Erupting volume: max speed 380-400 km/sec, jet contributes to the acceleration.

Reconnection and jet emission following flux emergence

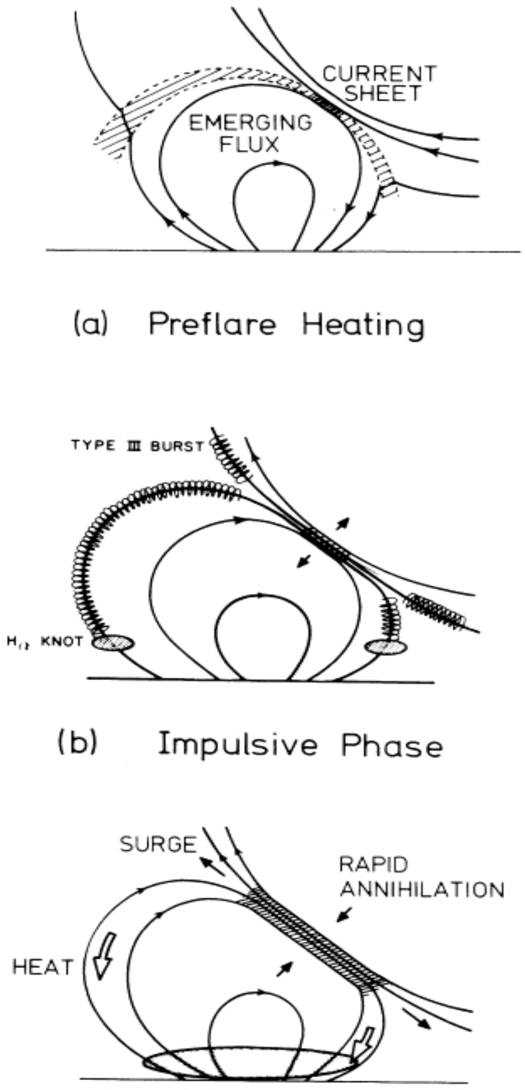

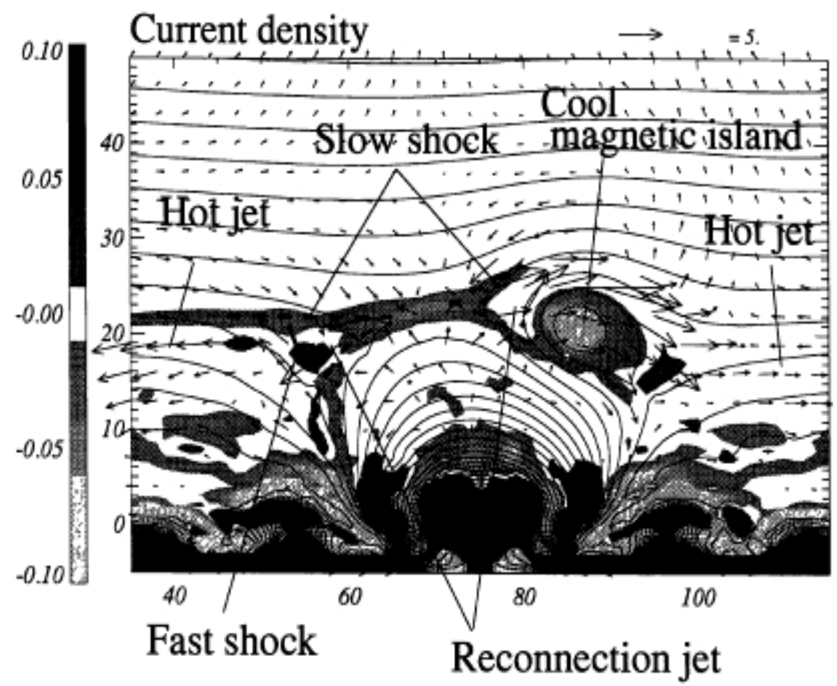

Yokoyama, T., Shibata, K. PASJ 48 (1996)

Heyvaerts, J., Priest, E., Rust, D. ApJ 216 (1977)

Coronal hole jets

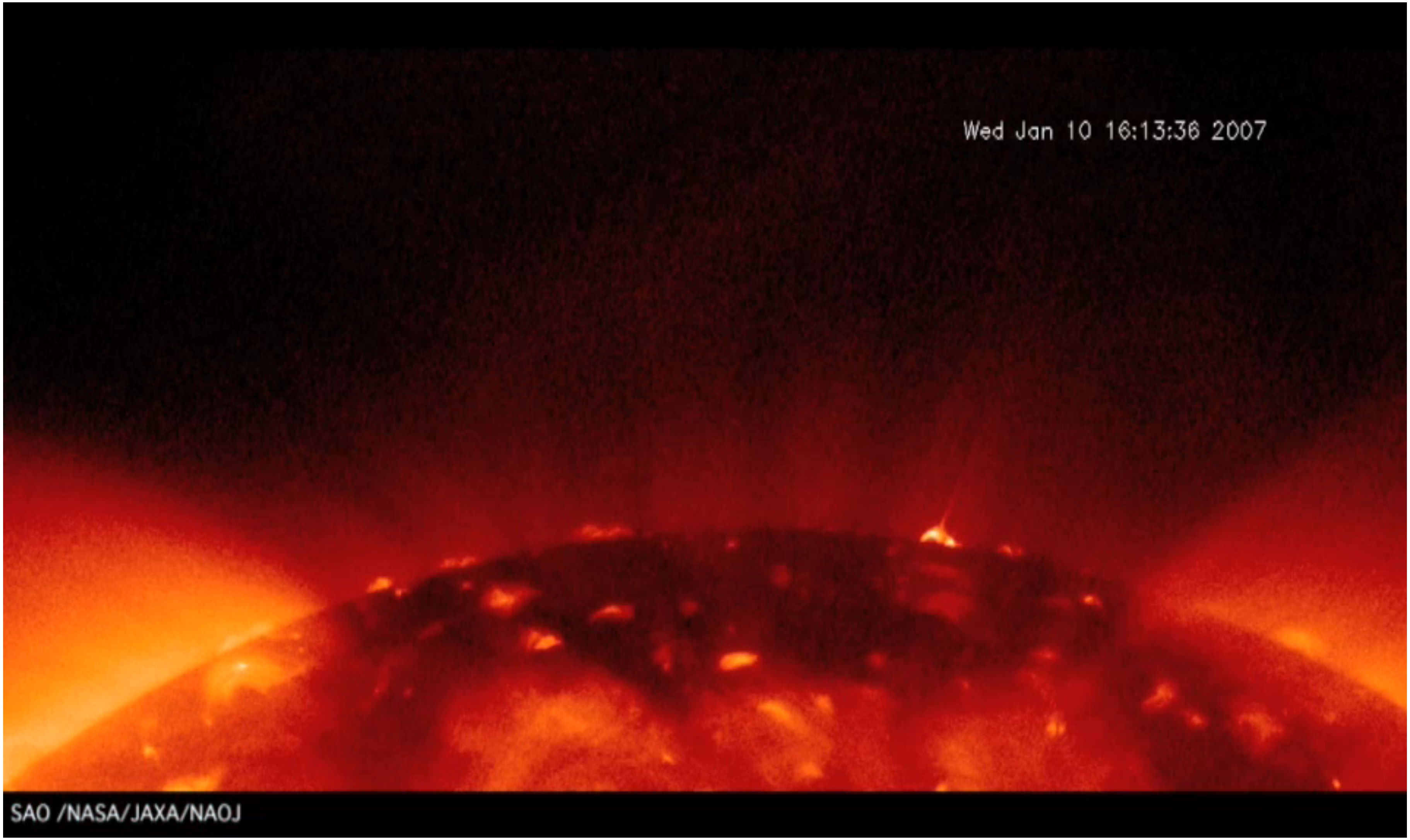

X-Ray telescope on Hinode. Northern coronal hole. Lots of jets!

Recurrent jets in ARs

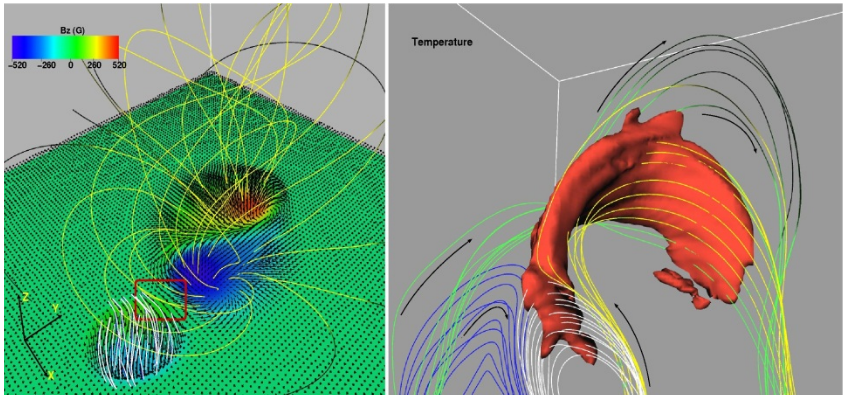

Gontikakis, C. et.al, A&A 506, (2010)

Archontis, V et.al, A&A 512, (2010)

Jets in coronal holes

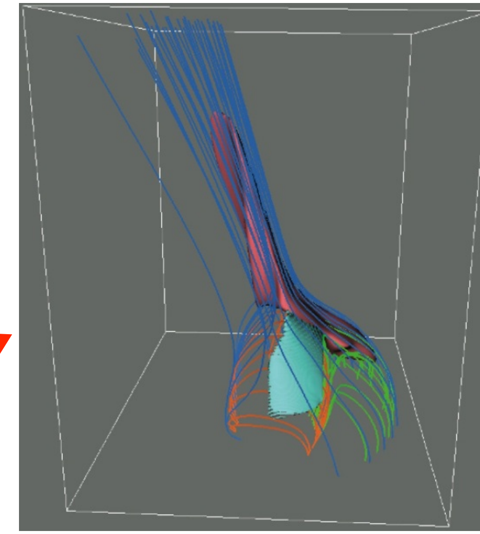

Moreno-Insertis et.al ApJ 673, (2008)

Jets

Helical polar coronal jets, STEREO

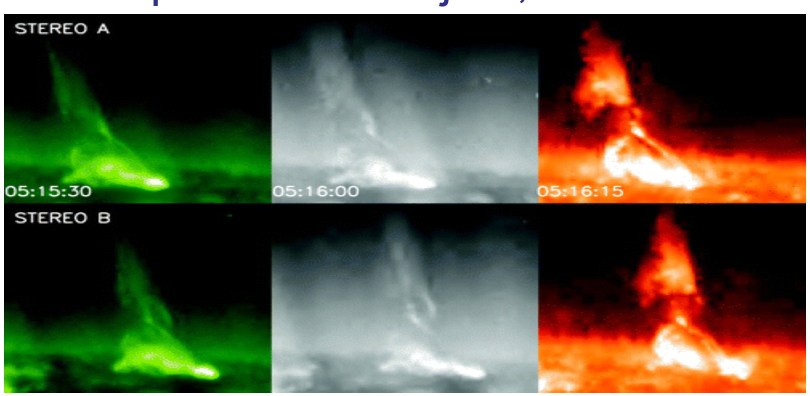

Patsourakos, S. et.al ApJ 680, (2008)

Giant chromospheric anemone jets

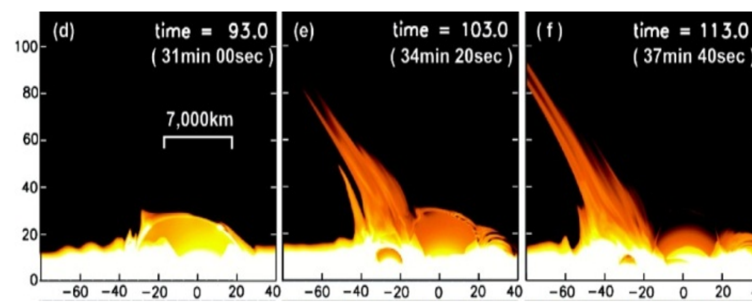

Nishizuka, N. et.al ApJ 683, (2008)

Ejection of dense plasmoids

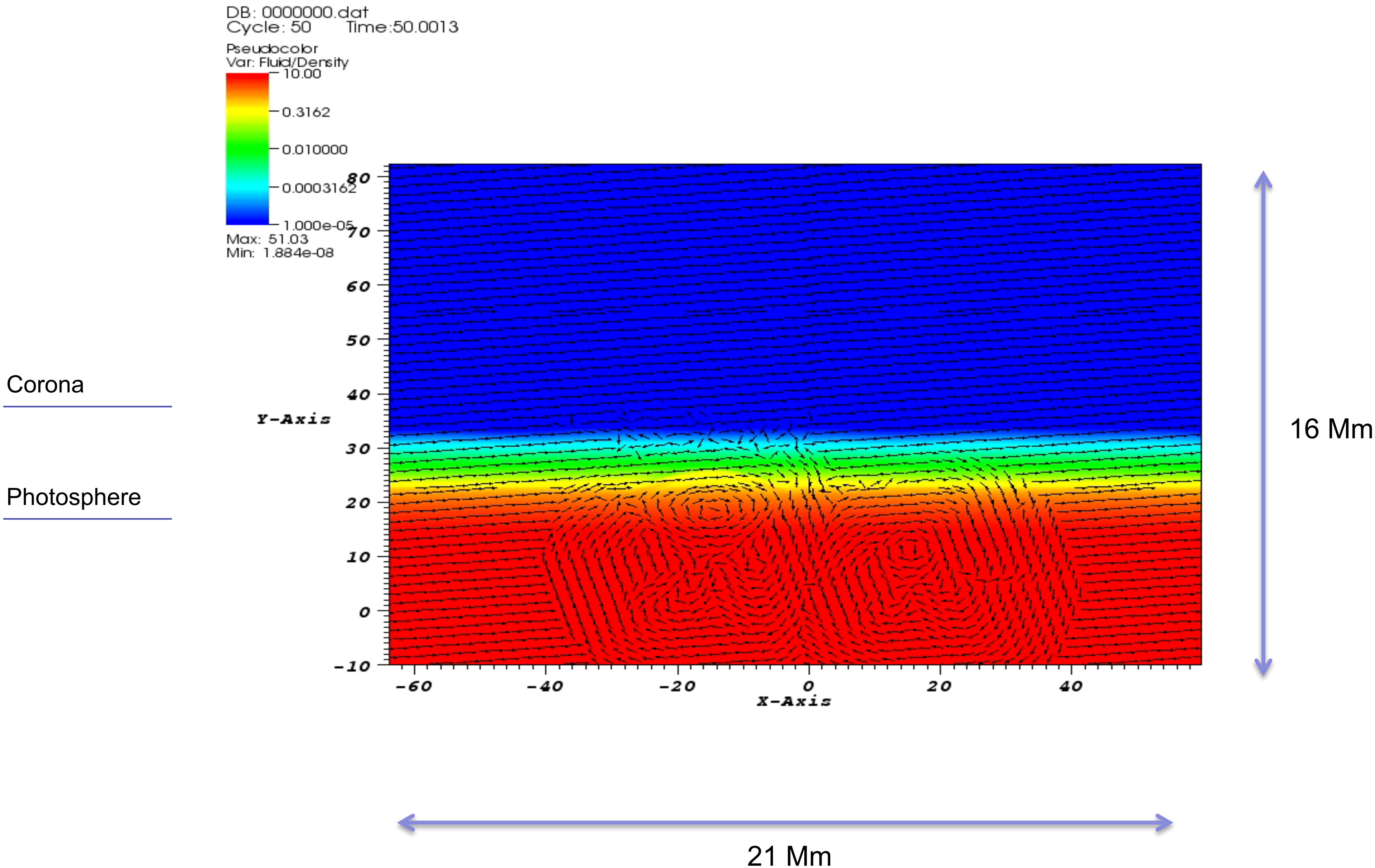

Heating and arcade-like structure

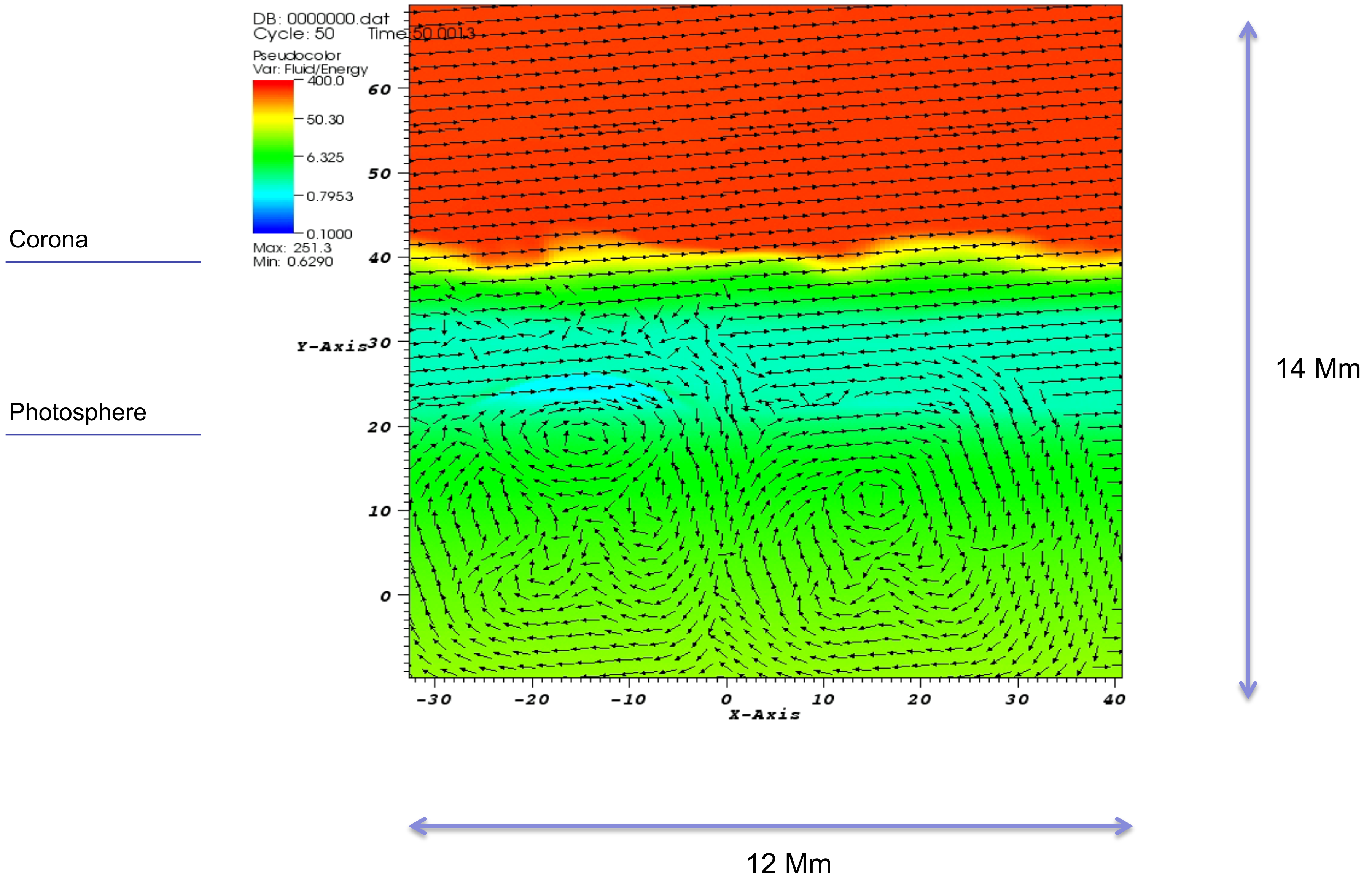

The development of complexity in ARs

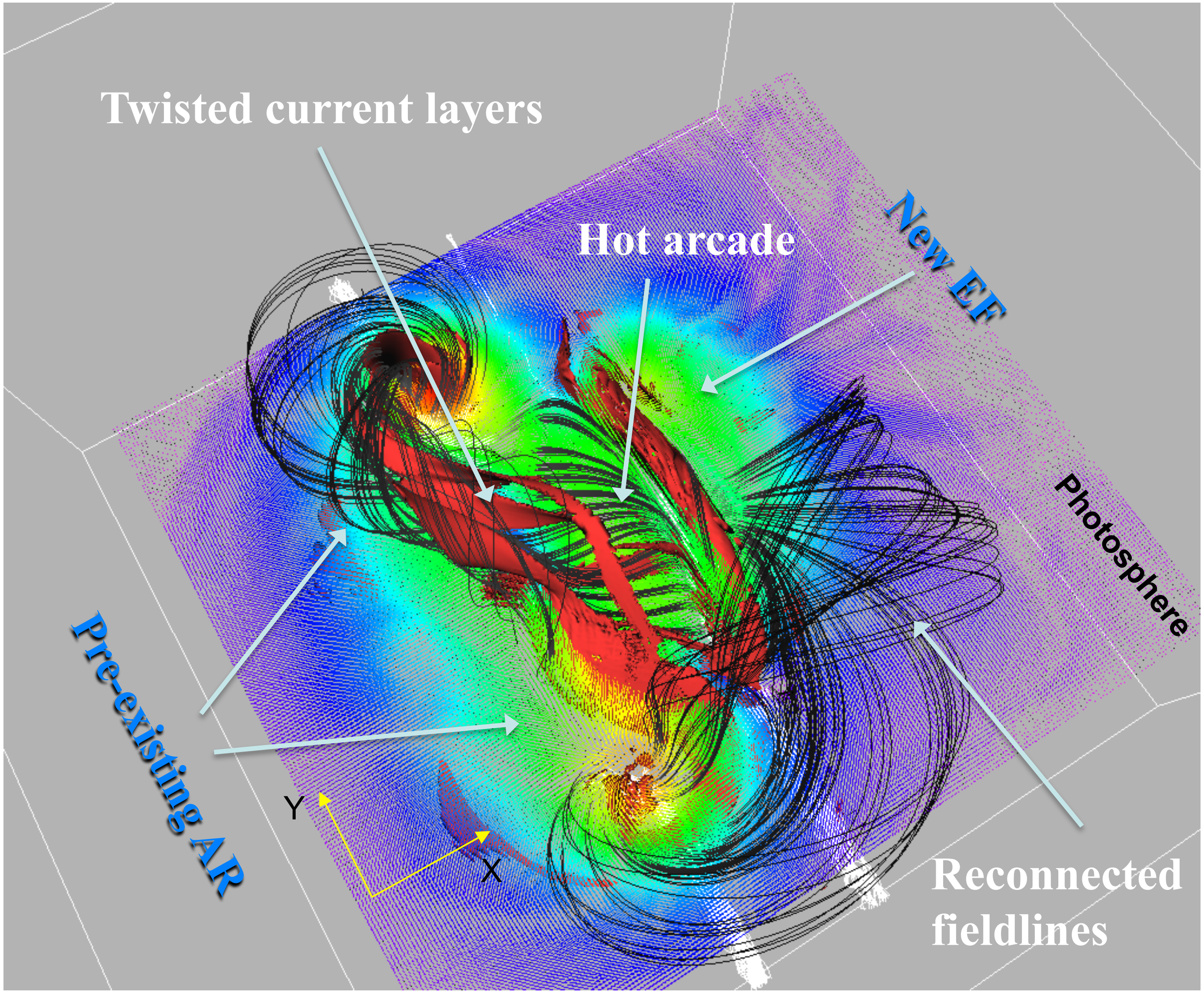

Summary

- SDO, Hinode, Stereo, Rhessi, Soho *revolutionised our understanding* of the solar magnetic activity.

- Many phenomena driven by newly emerging magnetic fields. Flux emergence is highly time dependent, has *complex* 3D geometry and contains *a wide range* of important length and time scales.

- Basic process of flux emergence now understood. It is *governed by the dynamics* of the emerging plasma. However*, thermodynamics* is needed for direct comparison with observations. Key ingredient is interaction with coronal field.

- Numerical models *have been successful* in re-producing a series of dynamical phenomena in the Sun (plasmoids, jets, sigmoids, eruption-like events).

- To understand how magnetic fields lead to the observable magnetic activity, it is essential to understand the transport of dynamo-generated nagnetic field to the solar surface, the formation of sunspots/ARs and the coupling with the outer atmosphere.